Ministry for Primary Industries
Manatū Ahu Matua

# Enteric methane mitigation through nanoparticles

MPI Technical Paper No: 2013/28

Prepared for the Ministry for Primary Industries
by AgResearch in partnership with PolyBatics, Massey University and PGgRc

ISBN No: 978-1-77665-882-4
ISSN No:

August 2013

New Zealand Government

# Disclaimer

The information in this publication is for consultation only: it is not government policy. While every effort has been made to ensure the information in this publication is accurate, the Ministry for Primary Industries does not accept any responsibility or liability for error of fact, omission, interpretation or opinion that may be present, nor for the consequences of any decisions based on this information. Any view or opinion expressed does not necessarily represent the view of the Ministry for Primary Industries.

Requests for further copies should be directed to:

Publications Logistics Officer
Ministry for Primary Industries
PO Box 2526
WELLINGTON 6140

Email: brand@mpi.govt.nz
Telephone: 0800 00 83 33
Facsimile: 04-894 0300

This publication is also available on the Ministry for Primary Industries website at http://www.mpi.govt.nz/news-resources/publications.aspx

# Contents

Page

**Executive Summary** **2**

**Introduction** **3**

**Results** **5**

**Milestone 1: Display of archaeal proteins on PHA nanobead surfaces** **5**

Create fusion proteins of the archaeal lytic enzyme PeiR and the PHA synthase PhaC. 5

Validate correct gene fusions by re-sequencing 6

Validate nanobeads produced by the fused synthase enzyme through surface protein profiling and/or peptide fingerprinting 6

**Milestone 2: Specificity and activity against pure methanogen cultures** **9**

Specific binding capacity and enzymatic activity of PeiR-nanobeads will be quantified against *Methanobrevibacter ruminantium* M1. 9

Inhibition of methane production via PhaC-PeiR nanobeads 15

Effect of nanobead purification on biological activity and methane inhibition 17

**Milestone 3: The half-life of PHA nanobeads** **20**

The half-life of PeiR-displaying nanobeads will be determined in pure methanogen cultures using direct fluorescence light microscopy assays 20

The half-life of PeiR-displaying nanobeads will be determined in mixed methanogen cultures using direct fluorescent light microscopy assays 21

The long-term stability of PhaC nanobeads will be determined in RM02 medium and clarified rumen fluid 22

**Milestone 4: Evaluation of small molecule inhibitor (SMI) uptake** **23**

Small molecule inhibitors emerging from the chemogenomics programmes or already-published inhibitors will be evaluated *in silico* for nanobead uptake. Degrees of uptake will be correlated to known physicochemical SMI properties. 23

Suitable candidates will be tested for incorporation into nanobeads *in vitro* 26

**Summary and next steps** **28**

# Executive Summary

Methane emissions from livestock comprise about 30% of New Zealand's national total greenhouse gas emissions and New Zealand has played a pivotal role in spearheading ruminant methane mitigation research worldwide in both governance and science. At the forefront of this effort are several research programs that are attempting to inhibit specific methane producing microbes (methanogens) in the rumen.

These programmes will require an effective, cost-efficient and non-toxic (environmentally friendly) delivery mechanism that specifically seeks out and targets rumen methanogen cells while providing a protective mechanism for a variety of methanogen inhibition compounds against the harsh rumen environment. We aim to achieve this by utilising bioplastic nanobeads as a cost efficient delivery vehicle, where surface displayed methanogen binding proteins, antibodies and internally bound small molecule inhibitors will specifically seek out, bind to, and inhibit rumen methanogens *in vivo*.

In this one year SLMACC pilot project we demonstrated that an archaeal lytic enzyme, PeiR, could be functionally displayed in full length as a C-terminal protein fusion to the polyhydroxyalkanoate synthase PhaC on the surface of PHA nanobeads while retaining its biological anti-methanogen activity. Lytic activity was measured in growth assays and confirmed not only for the host strain *Methanobrevibacter ruminantium* M1, but also for *Methanobrevibacter sp.* AbM4, and, to a lesser degree, *Methanobrevibacter olleyae* 229-11. Furthermore, lytic activity of PhaC-PeiR nanobeads against *M. ruminantium* M1 was validated via direct fluorescence microscopy. PhaC-PeiR nanobeads inhibited methane production in pure cultures up to 100% for *M. ruminantium* after 24 hours, 33% for *Methanobrevibacter sp.* AbM4 and 21% (after 48 hours) for *Methanosarcina barkeri* CM1. A significant increase in the biological activity (growth inhibition) and methane reduction was achieved when the nanobead purification protocol was optimised. Growth inhibition of *M. ruminantium* M1 was observed seven days post nanobead addition. Similarly, 100% methane inhibition for up to four days (95% reduction on day seven) was realised by PhaC-PeiR beads extracted using the optimised protocol. The stability of PhaC and PhaC-PeiR nanobeads was tested in *M. ruminantium* M1 pure culture over four days and for *M. ruminantium* M1 - *Ruminococcus flavefaciens* FD1 co-cultures for 24 hours. In either scenario, no structural degradation of nanobeads was observed, nor could any detrimental effects on *R. flavefaciens* FD1 cell number or cell morphology be detected. The long term stability of PhaC nanobeads was tested in RM02 growth medium and non-sterile clarified rumen fluid. No loss of nanobead fluorescence was found after 49 days of incubation.

A literature survey has been carried out to evaluate the existing body of work on the uptake and release of inhibitory compounds by PHA nanobeads. Known inhibitors of rumen methanogens were then reviewed for their likely suitability in a nanobead mediated drug delivery system. Anthraquinone was identified as the best application based compound. The uptake of anthraquinone into PHA nanobeads was subsequently determined and up to 400 µg anthraquinone / mg nanobeads were found to be incorporated into beads.

The SLMACC programme was able to successfully demonstrate the creation and use of PhaC-PeiR tailored nanobeads as a methane mitigation tool.

Future research aims at validating the biological anti-methanogen activity of PhaC-PeiR nanobeads in rumen fermenters and in animal models. Further, a range of suitable displayed anti-methanogen proteins and enzymes, anti-methanogen antibodies and lipophilic small molecule inhibitors has already been selected to be tested for their respective anti-methanogen activities and host range.

# Introduction

New Zealand has emerged as one of the world leaders in agricultural Greenhouse Gas Mitigation. Many novel lines of research have been initiated, including the field of reducing methane emissions from ruminant livestock (methane contributes approximately 30% of New Zealand total greenhouse gas emissions). Most of these research streams aim at developing anti-methanogen compounds, proteins and vaccines that can be successfully used in a pastoral system. Research to date, however, has shown that the rumen is a highly complex and active environment with a high turnover rate. It is also specialised in fibre and protein breakdown, making the delivery of long-lived, stable anti-methanogen compounds to the rumen particularly challenging. This challenge must be met in order for nutritionally valuable meat and dairy products to continue to be produced in a sustainable manner.

Recent developments in the field of nanotechnology have resulted in the creation of biopolymer nanobeads. A number of microbes are capable of synthesizing polyhydroxyalkanoate (PHA) as carbon and energy reservoirs (29). The key enzyme for PHA biosynthesis is the PHA synthase PhaC (60) which forms the polyester by linking *(R)*-3-hydroxyacyl-CoA thioester. The resulting biopolymer remains covalently bound to PhaC. The hydrophobic polyester strands aggregate into spherical nanobeads with the strands in the core and attached proteins forming the surface (Figure 1).

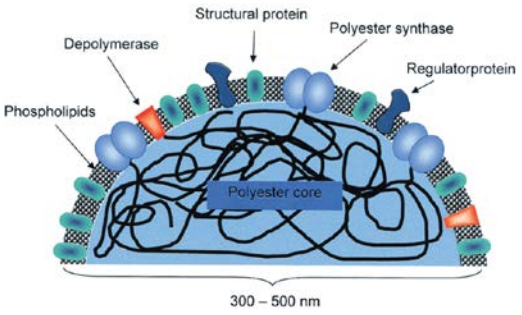


**Figure 1: schematic composition of a PHA nanobead [from Rehm, B. H. A. Biochemical Journal 2003]**

We hypothesised that by using biopolymer nanobeads as a delivery vehicle (12), we can successfully administer three anti-methanogen strategies to the rumen environment at once. Firstly, methanogen binding proteins and antibodies, displayed on the surface of the beads, will specifically seek out and bind to rumen methanogens *in vivo*, thus causing steric inhibition of methanogen activity. Secondly, these bound nanobeads will create a microenvironment where other surface bound anti-methanogen enzymes, such as lytic enzymes able to degrade the methanogen cell wall, are brought in close vicinity to methanogen cells. Thirdly, lipophilic small molecule inhibitors can be loaded into the interior of the nanobeads and slowly released over time (58), effectively turning the nanobeads into micro-boluses. Because of the minimized spatial distance between loaded nanobeads and methanogen cells we further hypothesise that the overall dosage levels for inhibitors required for rumen methanogen inhibition will be greatly reduced compared to direct-feed applications.

Nanobeads have proven to be effective, cost-efficient (as low as ~$USD6/kg pure beads) (12) and non-toxic (40) in previous studies. They can make up to 80-90% of the cell's dry weight (45). These structures currently receive significant biotechnological interest in a wide range of applications, including agriculture (29, 39, 40). Recently, polyhydroxyalkanoate, the main component of one type of nanobeads produced by recombinant cell factories, has gained FDA approval as a food additive (45). It has also been shown that the key enzyme, PhaC, tolerates protein fusions to both its C- and N-terminus (25, 44) and is able to display those fusion proteins on the nanobead surface (43). When those inclusion bodies are degraded in the rumen, they will release poly-hydroxy butyric acid and its monomer 3-hydroxy butyric acid (personal communication, Dr. Mike Tavendale). This butyric acid is likely to be taken up *in vivo* by the rumen epithelium and directly oxidised, supplying additional nutrients for the animals (14).

*Thus, we aim to use nanobeads to develop an effective, cost-efficient and non-toxic (environmentally friendly) anti-methanogen delivery mechanism (45, 46) that 1) specifically seeks out and targets rumen methanogen cells, and 2) provides a protective mechanism for a variety of methanogen inhibition compounds against the harsh rumen environment.*

There are a number of key advantages to this approach:

(1) Nanobeads displaying proteins are produced within microbial cells in a one-step process that does not require any physical or biochemical modification beyond a basic cell disruption to free the nanobeads. This implies cost effective large scale production of individual nanobead types.

(2) Lipophilic payloads such as certain small molecule inhibitors are incorporated into the nanobeads simply by adding the compound. Previous research has already investigated uptake and release kinetics for specific dyes (58) and these existing methodologies will be adapted for this research programme.

(3) Currently up to five different proteins can be displayed on the same bead. In combination with varying payloads, methanogens can be simultaneously targeted by more than one inhibition mechanism. This will significantly reduce the development of resistance to individual mitigation approaches. Furthermore, the use of methanogen binding proteins will bring internal payloads in close proximity to their intended target cells, increasing inhibitor efficiency and avoiding dilution and non-specific adsorption in the rumen. Less inhibitor will be required to achieve the same level of activity, further reducing product cost.

(4) The use of methanogen binding proteins (such as lytic enzymes that bind to and degrade the cell wall, proteins featuring pseudomurein binding domains, or methanogen specific antibodies) will create a primary inhibitory effect through steric inhibition, similar to the effect that pure antibodies originating from the vaccine programme will have on rumen methanogens.

(5) We hypothesize that the use of multiple anti-methanogen mechanisms on a single bead creates a significant synergistic effect, increasing the overall level of effectiveness beyond what individual components would achieve.

(6) Individual isolated anti-methanogen compounds and proteins could be subjected to rapid degradation in the rumen. By linking surface structures to larger bead structures and protecting small molecule inhibitors in the lipophilic bead interior, the stability of each active compound will be greatly increased.

(7) No recombinant DNA is a part of nanobeads, eliminating the risk of unwanted genetic transfer and reducing regulatory hurdles.

(8) Nanobead production and application is environmentally friendly. No toxic (by-) products are created or released during production, application and breakdown in the animal. In the rumen, the nanobeads are degraded into amino acids and fatty acids. These degradation products can then be taken up by the animal as nutrients.

(9) Previous research (5, 43) has shown that nanobeads and their surface attached functional enzymes are environmentally stable beyond 14 days. This will significantly increase the number of suitable and effective delivery mechanisms (e.g. drenches, boluses, salt licks, sprays on feed or water supplements). In particular, passive delivery mechanisms, such as a supplement in the animal's water supply, are inexpensive and promise a continuous and lasting reduction of rumen methanogens.

In this pilot study, the lytic enzyme PeiR of an integrated pro-virus (phi mru) found in the genome of *Methanobrevibacter ruminantium* M1 was chosen to investigate whether archaeal proteins and enzymes can be displayed on PHA nanobeads while retaining their specific native activities. As mentioned above, the rumen is a highly active system specialised on plant fibre breakdown. To gain a first insight in their potential lifetime and structural integrity, PHA nanobeads were subjected to in pure and mixed rumen microbial cultures and tested against clarified rumen fluid. Finally, uptake of the known hydrophobic methanogen inhibitor anthraquinone into PHA nanobeads was investigated.

# Results

## MILESTONE 1: DISPLAY OF ARCHAEAL PROTEINS ON PHA NANOBEAD SURFACES

### Create fusion proteins of the archaeal lytic enzyme PeiR and the PHA synthase PhaC.

The DNA sequence encoding for the predicted lytic enzyme PeiR from *M. ruminantium* M1 (Figure 2, Lysis module) was codon optimised for expression in *Escherichia coli* and synthesised by GeneArt (Germany).

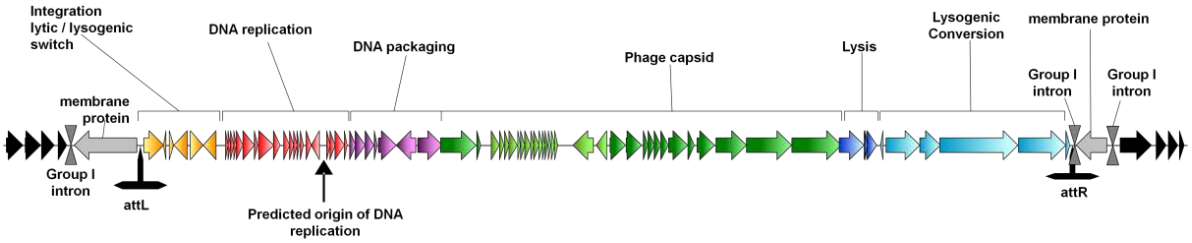


**Figure 2: Schematic representation of the *M. ruminantium* M1 integrated provirus genome of φmru.** Coding regions are shown as arrows, with predicted functional modules color coded. Attachment sites are shown as inverted 'T' (*attL* and *attR*).

A C-terminal protein fusion with the aim to combine the PhaC synthase and the PeiR lytic enzyme into one bi-functional protein was designed (Figure 3 B) and carried out (the corresponding N-terminal fusion was also designed and carried out in case no biological activity was obtained with the C-terminal construct (Figure 3 A, data not shown)). Briefly, custom oligonucleotides (5′- CTCGAGATGGTTCGTTTTAGCCGTGATATGC -3′ and 5′-GGATCCTTATGCCGGACACACAACATAATAATTCTGG-3′) containing the respective appropriate *Xho*I and *Bam*HI restriction sites were designed. The codon-optimised *peiR* gene was amplified using Platinum PCR SuperMix High Fidelity (Life Technologies Auckland, NZ) and TA-cloned into the pCR2.1 vector (Life Technologies, Auckland, NZ). Resulting recombinant *E. coli* colonies were selected, plasmid DNA isolated and subsequently sequenced. Plasmids with validated DNA insert sequences were then digested with *Xho*I and *Bam*HI to excise the *peiR* fragment. The *peiR* DNA fragment was subsequently gel purified and ligated into the similarly digested pET14b PhaC linker MalE plasmid (25) before transformation into *E. coli* XL1 Blue (Stratagene) cells for screening.

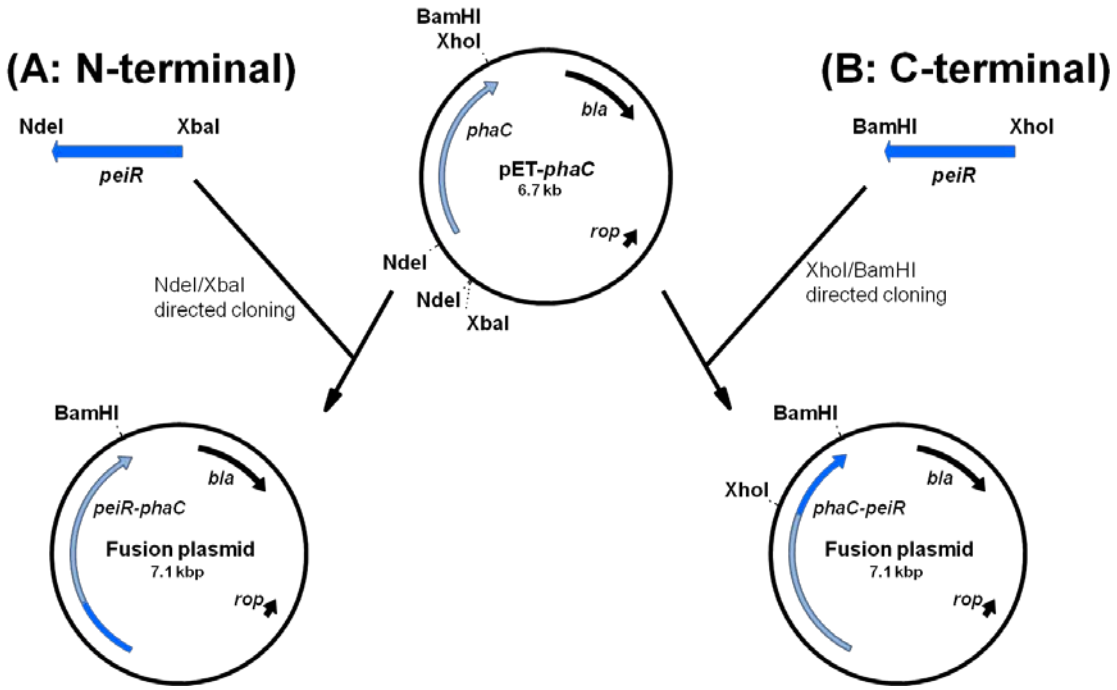


**Figure 3: Cloning scheme for (A) N-terminal and (B) C-terminal in-frame fusion of PeiR to PhaC using site-directed cloning.** The respective source pET-phaC vectors differ in their respective restriction sites for N- and C-terminal fusions. Gene fusion partners (e.g. *peiR*) are shown in blue, the plasmid bound PHA synthase, *phaC*, is depicted in light blue.

### Validate correct gene fusions by re-sequencing

The fusion *phaC-peiR* gene fusion plasmid was then verified via PCR amplification and direct sequencing (Allan Wilson Centre, Massey University (www.allanwilsoncentre.ac.nz)). The resulting DNA sequence reads were analysed for single nucleotide polymorphisms and correct in-frame ligation. The respective N-terminal fusion construct, resulting in a *peiR-phaC* in-frame gene fusion has been sequenced and verified (data not shown).

### Validate nanobeads produced by the fused synthase enzyme through surface protein profiling and/or peptide fingerprinting

The resulting *phaC-peiR* fusion gene plasmid was used to transform *E. coli* BL21 λ(DE3) competent cells which contained the helper plasmid pMCS69 (1). The helper plasmid pMCS69 is necessary for the production of *R*-3-hydroxybutyryl-coenzymeA (CoA) required for polyester bead synthesis. Similarly, control beads comprised of the native PHA synthase PhaC were produced by the plasmid pETC in *E. coli* BL21 λ(DE3). Briefly, *E. coli* containing the pET14bPhaC linker PeiR or pETC plasmids were grown in LB broth supplemented with ampicillin, chloramphenicol and 1 % glucose at 37 °C until an OD of 0.5 was reached before induction with 1 mM IPTG followed by shaking at 25 °C for 48 hours. Polyester granules containing PhaC-PeiR or control granules (PhaC only) were produced from the *E. coli* by sonication in a Vibracell sonicator (Sonics and Materials, CT, USA) on ice at power level 2 at 40 % duty for 20 s bursts over a 10 min time period with 30 s rest intervals. The granules were further purified by ultracentrifugation over a glycerol gradient as previously described (6) (Figure 4). Beads were resuspended in PeiR buffer (20 mM 3[-N morpholino]-propane sulfonic acid (MOPS) pH 7.0, 1 mM DTT, 0.3 M NaCl, 20 % glycerol) and stored at -80 °C. Polyester beads inside the bacterial cells were visualised with Nile Red staining described previously (2) and fluorescence microscopy.

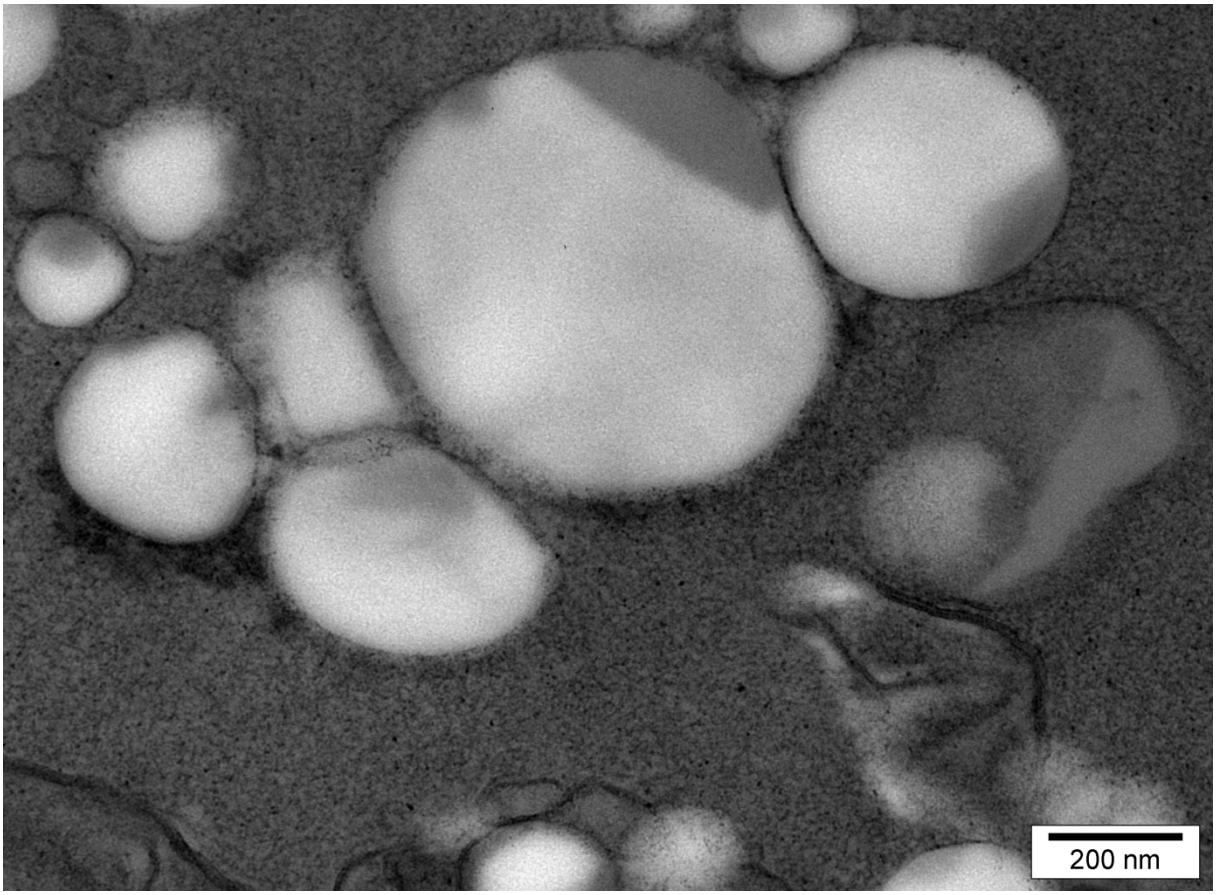


**Figure 4: Transmission electron micrograph of purified PhaC-PeiR nanobeads.** Beads assume a spherical shape and vary in size between 50 and 500 nm.

Protein profiles of the PhaC-PeiR polyester beads were verified via SDS-polyacrylamide gel electrophoresis on 4-15% gradient acrylamide gels (Biorad). Gels were stained with Safestain (Life Technologies Auckland, NZ). A protein band at 75-80 kDa was observed (Figure 5). While the observed band was somewhat lower than the expected 90 kDa, deviations between expected and observed protein sizes on SDS-PAGE analyses are not uncommon for PhaC fusion proteins (Rehm, personal communication). Nevertheless, the plasmid present in the *E. coli* production strain was re-verified via PCR and DNA sequencing to contain the full length *peiR* insert.

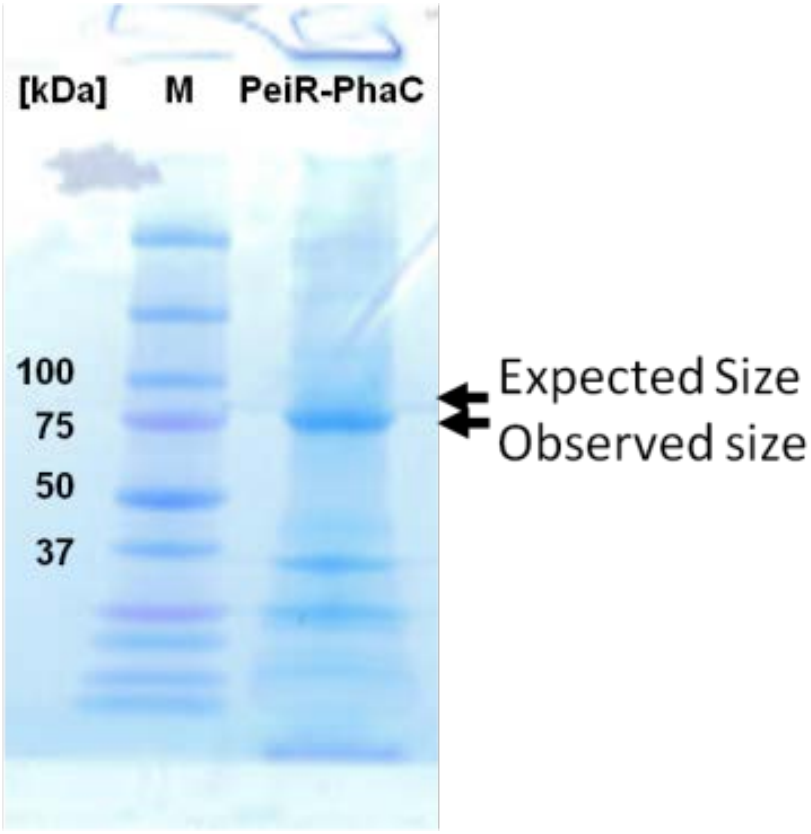


**Figure 5: Verification of the PhaC-PeiR fusion protein expression via SDS-PAGE**. SDS-PAGE of purified nanobeads. Lane M indicates the protein marker and lane PhaC-PeiR shows protein bands from a crude PhaC-PeiR nanobead purification. Black horizontal arrows mark the respective observed and expected protein sizes.

Subsequently, the corresponding PhaC-PeiR protein band from the SDS-PAGE gel was excised, trypsin digested and the subsequent peptides subjected to MALDI-TOF MS/MS peptide analysis (Dr. Stefan Clerens, AgResearch). Identified peptide fragments could be aligned to both PhaC and PeiR throughout their respective deduced amino-acid sequences (Figure 6). Despite the lower than expected SDS-PAGE protein band, the full-length fused PhaC-PeiR protein was shown to be present.

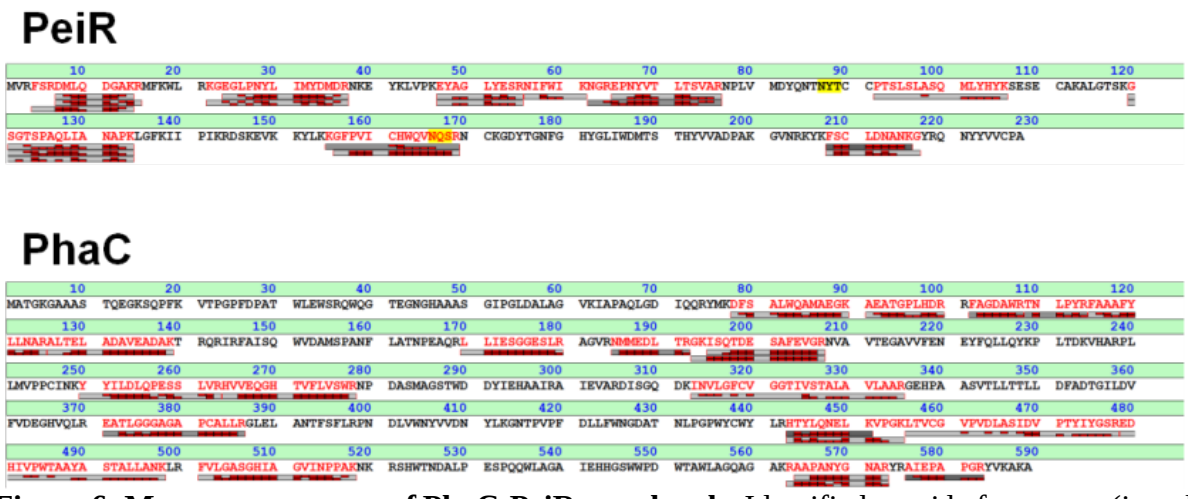


**Figure 6: Mass spectrometry of PhaC-PeiR nanobeads.** Identified peptide fragments (in red) were aligned against the deduced amino acid sequences of PeiR and PhaC.

## MILESTONE 2: SPECIFICITY AND ACTIVITY AGAINST PURE METHANOGEN CULTURES

Specific binding capacity and enzymatic activity of PeiR-nanobeads will be quantified against *Methanobrevibacter ruminantium* M1.

*Biological activity of PhaC-PeiR nanobeads against rumen methanogen strains using growth assays*

Lytic activity against microbes can be effectively measured by changes in the optical density (OD) of cultures growing in liquid media.

The enzymatic activity of PHA nanobeads displaying the lytic enzyme PeiR, was therefore measured in growth assays using *M. ruminantium* M1 as the host strain. In those assays the ability of PeiR to inhibit methanogen growth by degrading the pseudomurein cell wall was quantified. Two controls were employed: (i) *M. ruminantium* M1 cells without added nanobeads and (ii) PhaC nanobeads added to *M. ruminantium* M1 cells. The biological activity of PhaC-PeiR nanobeads was then assessed by addition to growing *M. ruminantium* M1 cells. Briefly, RM02 media was inoculated with 1 % growing methanogen culture and cell growth monitored over time by measuring $OD_{600}$. At the beginning of the exponential growth phase ($OD_{600}$ ~0.1), 10 mg PhaC control or PhaC-PeiR beads suspended in 100 µl of buffer was added to the cell suspension and changes in $OD_{600}$ recorded over time.

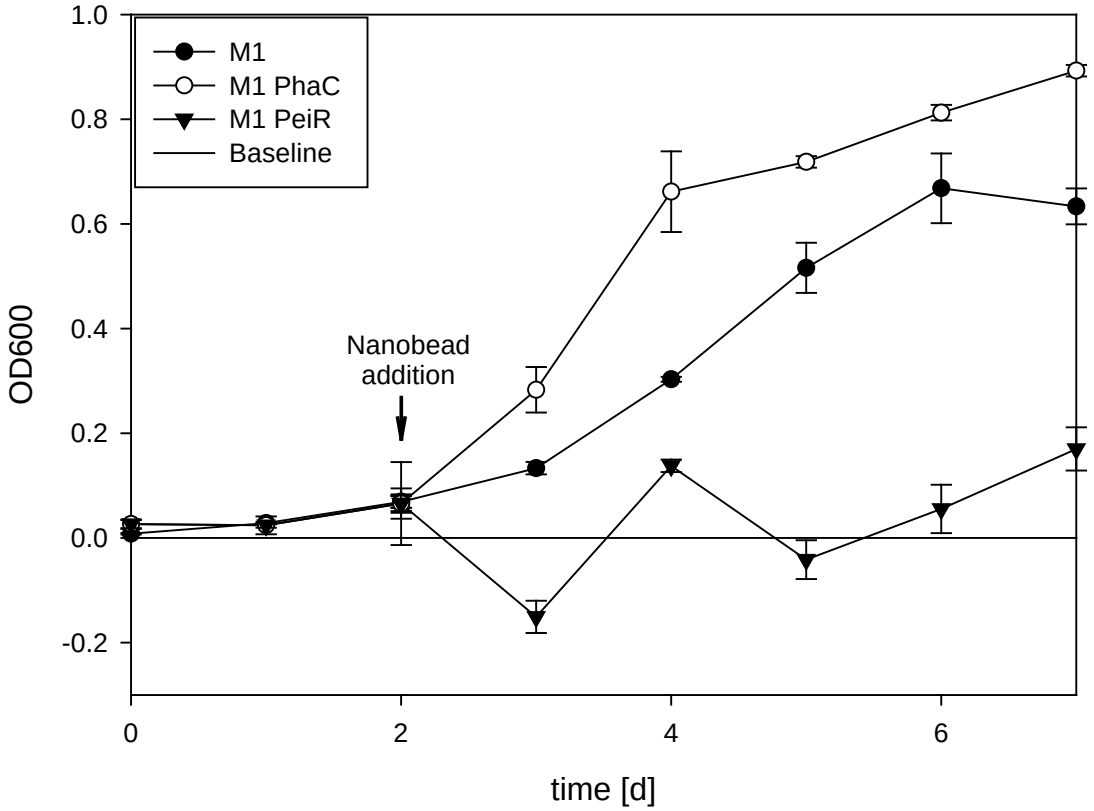


**Figure 7: Optical density assay testing the effect of PhaC-PeiR nanobeads on *M. ruminantium* M1.** M1: control (i), *M. ruminantium* M1 cells only; M1 PhaC: control (ii), *M. ruminantium* M1 plus PhaC nanobeads; M1 PeiR, *M. ruminantium* M1 with added PhaC-PeiR nanobeads; baseline: visual reference line for OD600 = 0; vertical arrow, time point of nanobead addition. The assay was carried out in triplicate. Optical densities were corrected as described. Error bars represent the standard error calculated from uncorrected measured optical density values.

Figure 7 representatively shows the effect of PhaC-PeiR nanobeads on growing *M. ruminantium* M1 cultures. While the addition of PhaC nanobeads consistently resulted in an increased optical density compared to the control without nanobeads, PhaC-PeiR nanobeads effectively inhibited cell growth over five days. The assay was independently repeated three times and the activity of PhaC-PeiR nanobeads was confirmed throughout. Statistical analyses were carried out using four independent experimental repetitions. Significant reductions in optical density were found (p-value <=0.05) for all days but day 4 using repeated measure (Figure 8 A) and for all days post nanobead addition using a regression analysis (Figure 8 B).

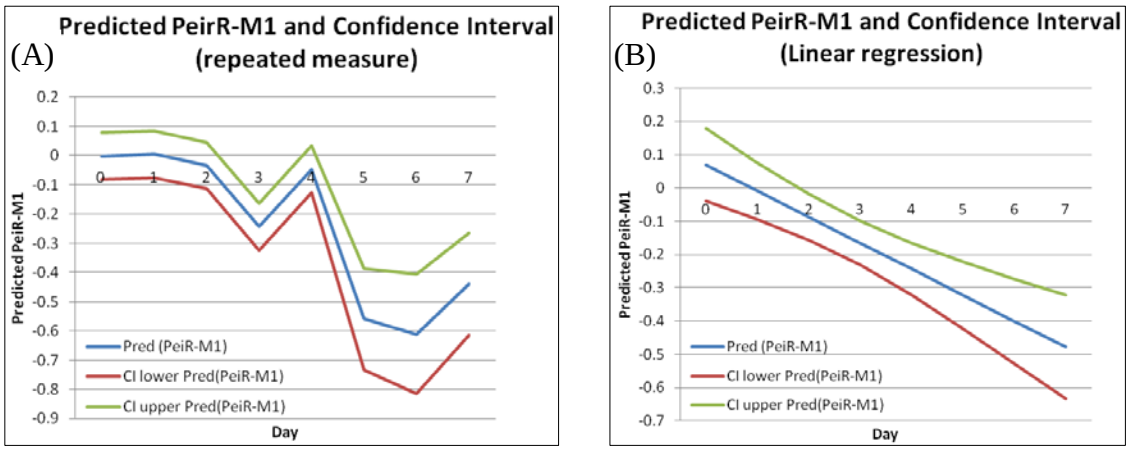


**Figure 8: Statistical evaluation of the significance of the addition of PhaC-PeiR nanobeads to *M. ruminantium* M1 cells in growth assays when compared to M1 cells.** (A) Repeated Measure analysis, (B) Linear regression analysis. 'CI': Confidence Interval. Statistical analyses were carried out by Lindy Guo (AgResearch Ltd).

A number of parameters were taken into account to correct the measured optical densities: (i) the addition of nanobeads to the cell suspension increases the optical density significantly ($\Delta_{ODnanobeads} = OD_{post\text{-}nanobeads} - OD_{pre\text{-}nanobeads}$) and (ii) PhaC-PeiR nanobeads exhibit a decrease in optical density over time, most prominently during the first 24 hours after addition to the growing *M. ruminantium* M1 cells ($OD_{bead(t-1)} - OD_{bead(t)}$). Interestingly, PhaC nanobeads remained stable over the entire assay. Optical densities were therefore corrected as follows:

$$OD_{corrected(t)} = OD_{measured(t)} - (\Delta_{ODnanobeads}) + (OD_{bead(t-1)} - OD_{bead(t)})$$

The substantial biological activity of PhaC-PeiR nanobeads against the original host strain *M. ruminantium* M1 led to the hypothesis that a greater range of phylogenetic different rumen methanogen strains may be susceptible to this tailored nanobeads variant.
The enzymatic activity of PhaC-PeiR nanobeads was therefore further evaluated for *Methanobrevibacter sp.* AbM4, *Methanobrevibacter olleyae* 229-11, and *Methanobacterium formicicum* BRM9 (Figure 9 A, B, and C, respectively).

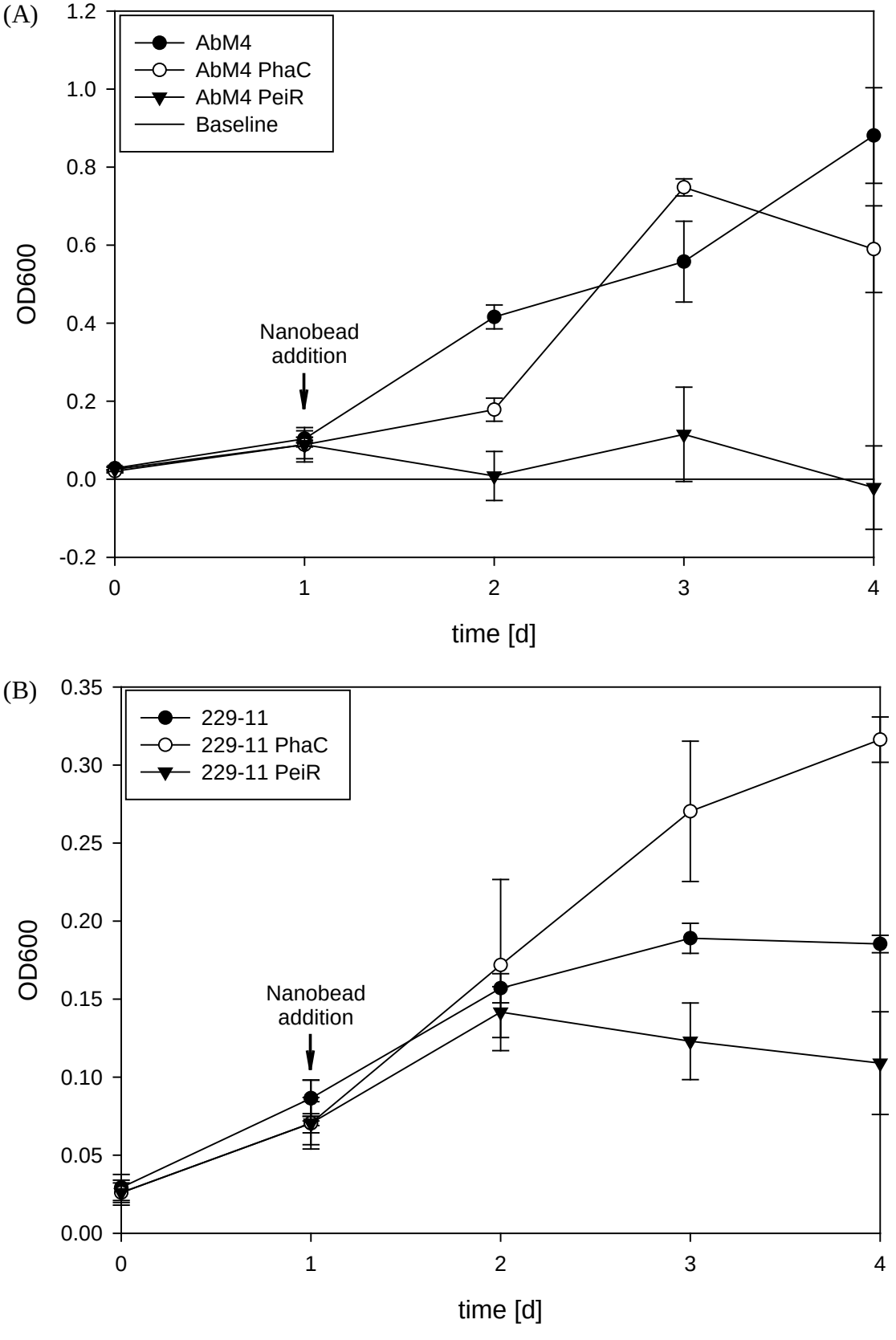

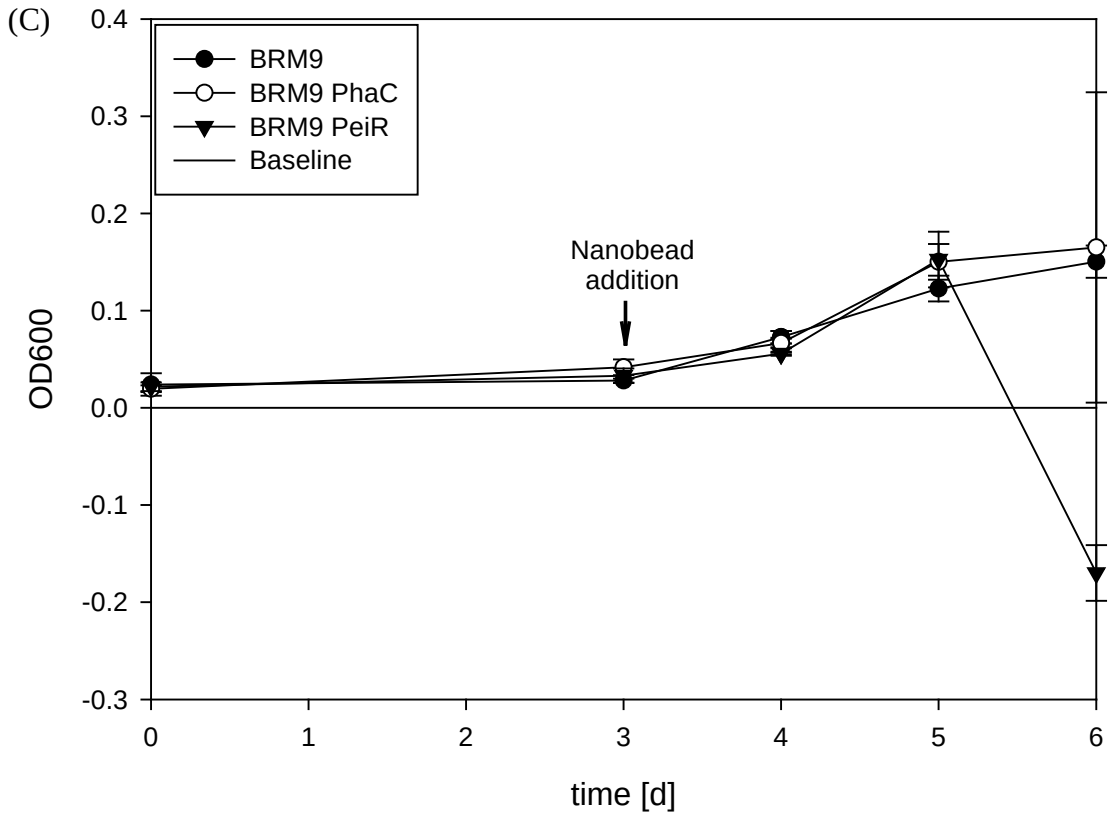


**Figure 9: Optical density assay testing the effect of PhaC-PeiR nanobeads on *Methanobrevibacter sp.* AbM4, *Methanobrevibacter olleyae* 229-11, and *Methanobacterium formicicum* BRM9.** Control (i), cells only; PhaC: control (ii), cells plus PhaC nanobeads; PeiR, cells with added PhaC-PeiR nanobeads; baseline: visual reference line for OD600 = 0; vertical arrow, time point of nanobead addition. The assays were carried out in triplicate. Optical densities were corrected as described. Error bars represent the standard error calculated from uncorrected measured optical density values.

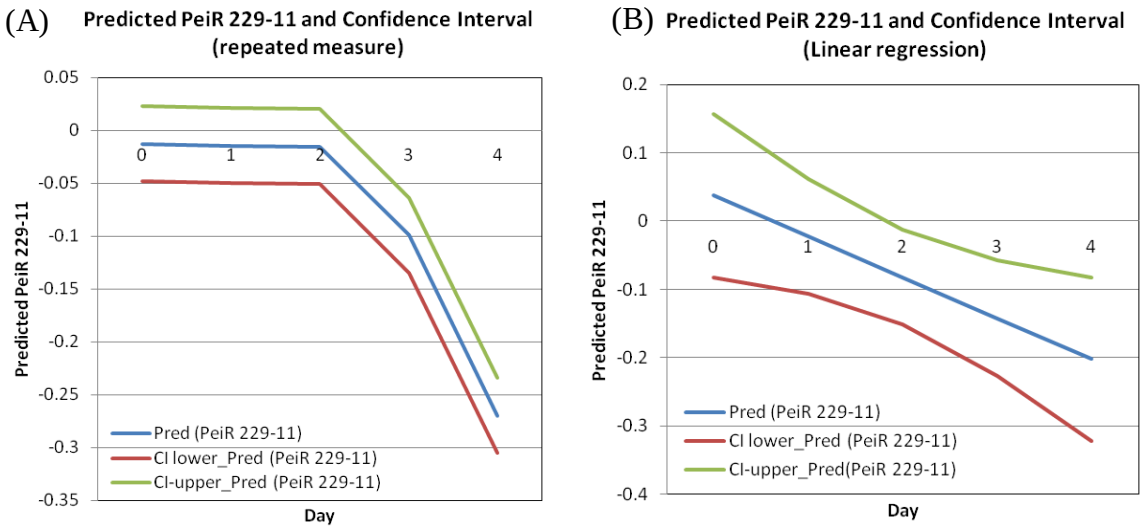


**Figure 10: Statistical evaluation of the significance of the addition of PhaC-PeiR nanobeads to *M. olleyae* 229-11 cells in growth assays when compared to 229-11 cells.** (A) Repeated Measure analysis, (B) Linear regression analysis. 'CI': Confidence Interval. Statistical analyses were carried out by Lindy Guo (AgResearch Ltd).

Similar to M1, *Methanobrevibacter sp.* AbM4 showed growth inhibition over the entire duration of the assay. Interestingly, *Methanobrevibacter olleyae* 229-11 inhibited a delay of 24 hr until growth inhibition was observed. This delay in OD-reduction was confirmed in an independent experimental repetition and may reflect changes in the cell surface structure of *M. olleyae* 229-11 that delay the action of PhaC-PeiR nanobeads. A statistical analysis comparing growing *Methanobrevibacter olleyae* 229-11 cells against 229-11 cells treated with PhaC-PeiR nanobeads showed a significant reduction in optical density for days 3 and 4 using repeated measure (Figure 10 A) and for days 2, 3 and 4 using a linear regression analysis (Figure 10 B). In contrast, *Methanobacterium formicicum* BRM9 appeared to be insensitive to the lytic enzyme PeiR displayed on PHA nanobeads for at least 48 hr. Similar to *M. olleyae*, further independent assays are required to investigate whether the observed loss in optical density after 72 hr is biologically significant or if this represents a systematic error in the assay for this organism.

Further experiments investigating the possible delayed action of PhaC-PeiR nanobeads against *Methanobrevibacter olleyae* 229-11 and *Methanobrevibacter olleyae* 229-11 are recommended to validate the biological relevance of the observed methanogen inhibition trends.

*Biological activity of PhaC-PeiR nanobeads against rumen methanogen strains using fluorescent microscopy*

Growth assays measure changes in optical density of a cell suspension, however, they do not directly demonstrate cell lysis.

To confirm *M. ruminantium* M1 cell lysis mediated through PhaC-PeiR nanobeads, presence and absence of *M. ruminantium* M1 cells was optically assessed using fluorescence light microscopy. PhaC and PhaC-PeiR nanobeads were loaded with the lipophilic dye Nile Red and added to growing *M. ruminantium* M1 cells as described above. The presence of M1 cells was then visualised using a Leica DM2500 Fluorescence Light Microscope (Figure 11 A and B, respectively).

(A)

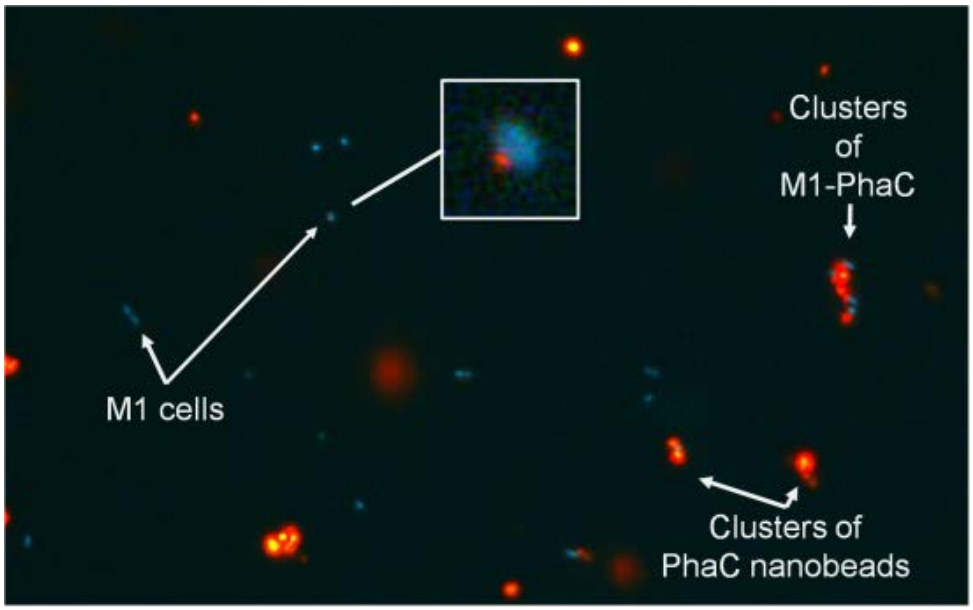


(B)

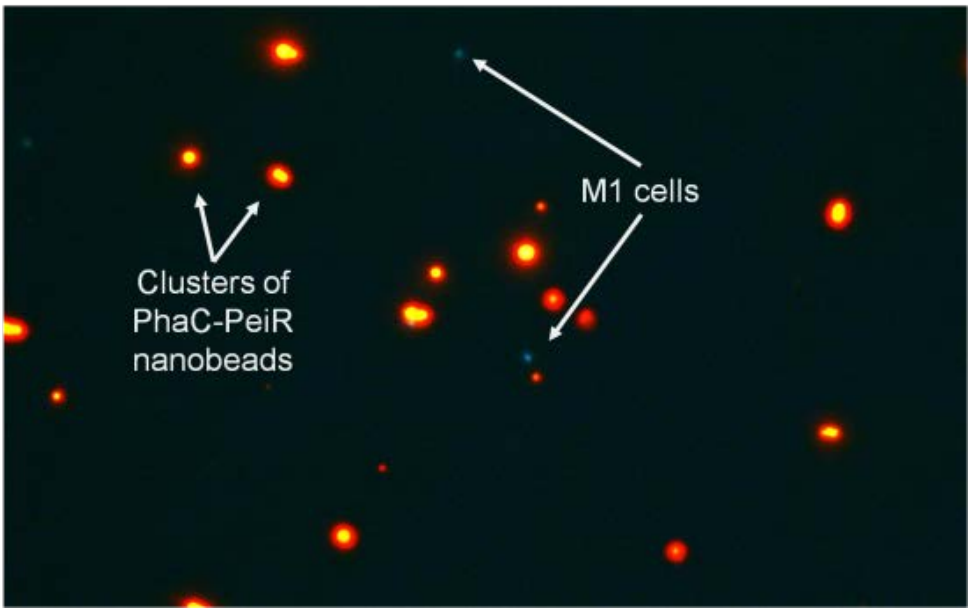


**Figure 11: Fluorescence micrographs of *M. ruminantium* M1 with PhaC (A) and PhaC-PeiR (B) nanobeads.** The inset in (A) depicts the co-existence of M1 cells and PhaC nanobeads.

While PhaC nanobeads did not lyse *M. ruminantium* M1 cells (Figure 11 A), almost no M1 cells were recovered when PhaC-PeiR nanobeads were present (Figure 11 B). This provided

direct visual evidence of cell lysis mediated by PhaC-PeiR nanobeads against *M. ruminantium* M1. It is interesting to note that in the presence of PhaC-PeiR nanobeads not all M1 cells were lysed. This phenomenon appears to be similar in nature to other anti-microbial strategies such as antibiotics, in that a small fraction of resistant cells may survive agent exposure. Here, a subset of M1 cells may exhibit a different cell surface makeup, such as variations in the glycocalyx, creating a (partial) resistance to the enzymatic action of PeiR. Further, Figure 11 B revealed that PhaC-PeiR nanobeads tend to form larger clusters when compared to PhaC nanobeads. These larger clusters may cloak a significant percentage of enzymatic activity by reducing the effective surface area available for PeiR display to methanogen cells. In line with these observations the nanobead extraction protocol was analysed with regard to the effects of the mechanical disruption of the production *E. coli* cells on nanbobead cluster formation. An alternative extraction protocol was developed and PhaC-PeiR activities compared (see below).

### Inhibition of methane production via PhaC-PeiR nanobeads

The goal of rumen methanogen inhibition is a reduction in methane emissions. While cell lysis is a good indirect indicator for likely reduced methane production, direct methane measurement assays were carried out to evaluate the effect of PhaC-PeiR nanobeads. Pure cultures of *M. ruminantium* M1, *Methanobrevibacter olleyae* 229-11, *Methanobrevibacter* sp. AbM4, *Methanobacterium formicicum* BRM9, and *Methanosarcina barkeri* CM1were mixed with PhaC and PhaC-PeiR nanobeads. Briefly, RM02 media was inoculated with 1 % of growing methanogen cultures and cell growth monitored by measuring $OD_{600}$ over time. At the beginning of the exponential growth phase ($OD_{600}$ ~ 0.1) 100 µl of PhaC control or PhaC-PeiR nanobeads beads (wet weight 10 mg) was added to the methanogen cultures. Immediately after bead addition, the culture headspace was flushed with hydrogen to remove any trace of methane present prior to bead inoculation and then re-pressurised with the appropriate gas mix. Methane produced by methanogens will diffuse into the growth medium and from there into the gaseous headspace. Amounts of methane present in the headspace were measured in 24 hour intervals by gas chromatography. After gas samples were taken, the headspace was flushed with hydrogen to remove any methane and enable an ongoing record of methane production. All experiments were performed in triplicate.

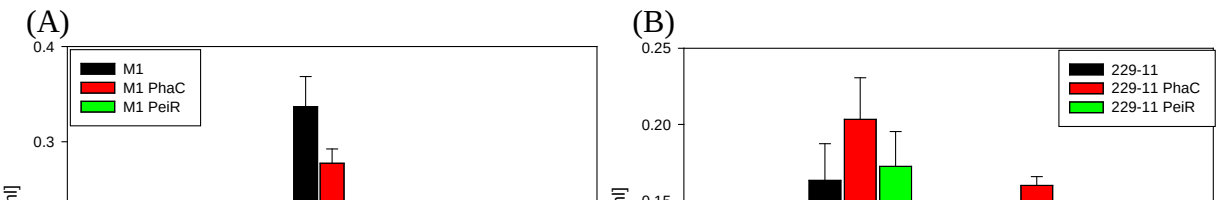

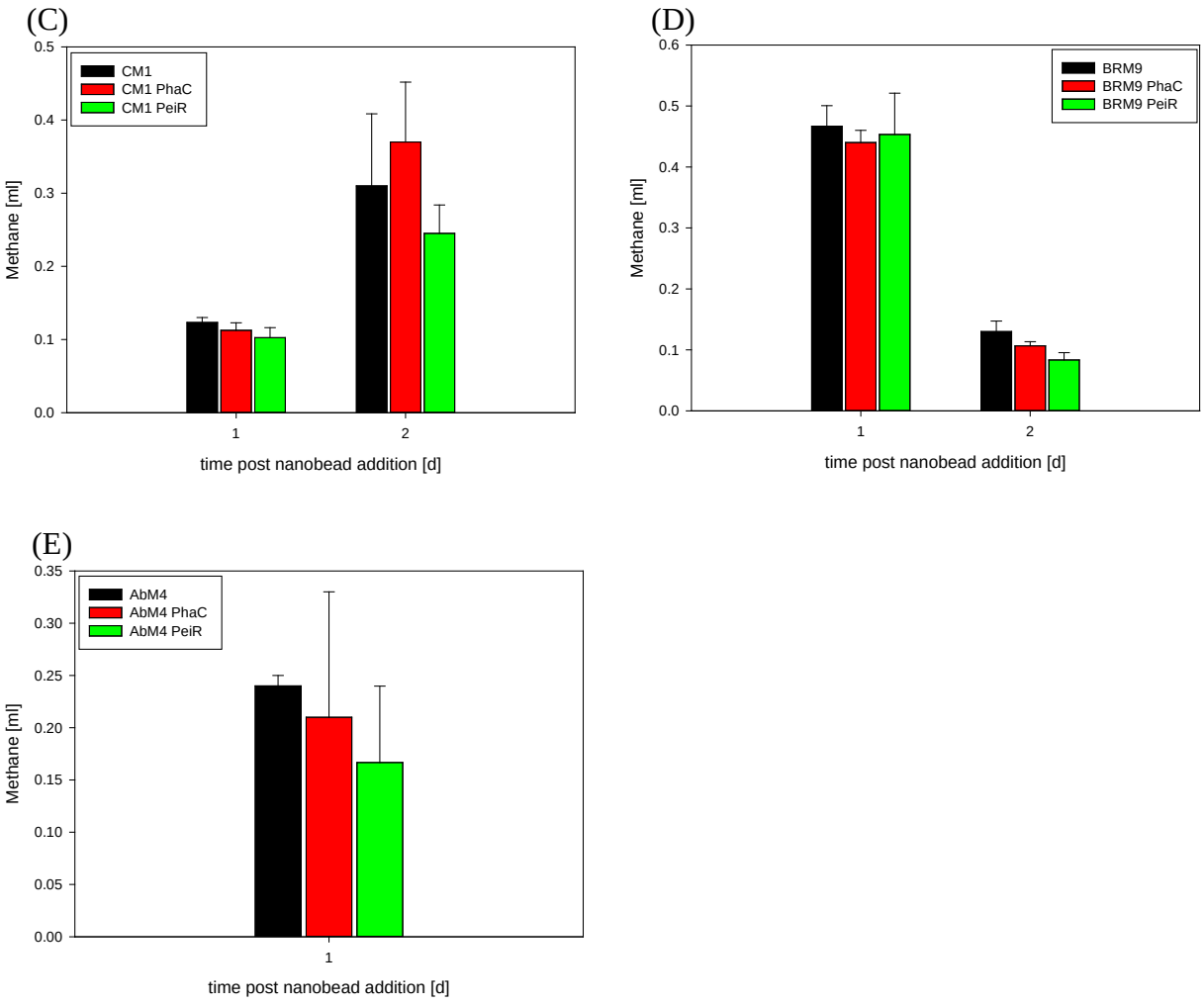


**Figure 12: Methane production in pure cultures in the presence of PhaC and PhaC-PeiR nanobeads.** Assays were carried out in triplicate. (A): *M. ruminantium* M1, (B): *Methanobrevibacter olleyae* 229-11, (C): *Methanosarcina barkeri* CM1, (D): *Methanobacterium formicicum* BRM9, and (E): *Methanobrevibacter* sp. AbM4. Error bars represent the standard error.

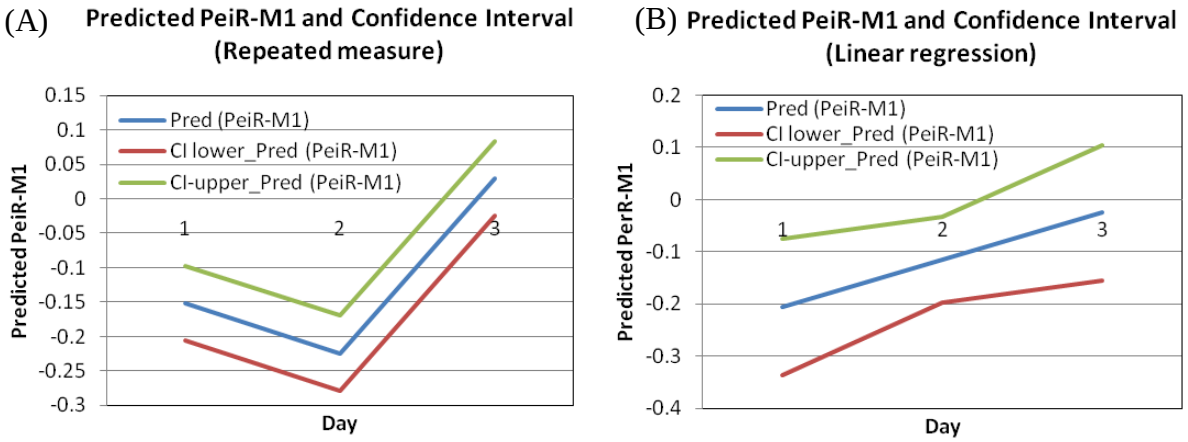


**Figure 13: Statistical evaluation of the significance of the addition of PhaC-PeiR nanobeads to *M. ruminantium* M1 cells in methane production assays when compared to M1 cells.** (A) Repeated Measure analysis, (B) Linear regression analysis. 'CI': Confidence Interval. Statistical analyses were carried out by Lindy Guo (AgResearch Ltd).

Methane was measured for up to three days after the addition of nanobeads. A reduction in methane production was observed for *M. ruminantium* M1 (100 % after 24 hours, 59 % after 48 hours; Figure 12 A), for *Methanobrevibacter sp.* AbM4 (33 % after 24 hours; Figure 12 E) and for *Methanosarcina barkeri* CM1 (and 21 % after 48 hours; Figure 12 C). No methane reduction was observed for *Methanobrevibacter olleyae* 229-11 and for *Methanobacterium formicicum* BRM9 (Figure 12 B and D, respectively).
It may be possible that the delayed inhibition shown in Figure 9 B and C reflects a delayed methane inhibition as well. Further methane inhibition measurements at later sample times are needed to test for delayed methane inhibition by PhaC-PeiR nanobeads. Interestingly, methane inhibition was also observed for *Methanosarcina barkeri* CM1 although this species has a different cell wall structure. It may be possible that PeiR displayed on PHA nanobeads weakly recognises and binds to cell surface compounds of CM1 and, similar to anti-methanogen antibodies, mediates a steric inhibition and thus a reduction in metabolic activity.

The methane production assay was independently repeated twice for *M. ruminantium* M1 and the activity of PhaC-PeiR nanobeads was confirmed throughout. Statistical analyses were carried out using both independent experimental repetitions. Significant reductions in methane production were found (p-value <=0.05) for days 1 and 2 post nanobead addition using repeated measure (Figure 13 A) and regression analyses (Figure 13 B).
The number of independent experimental repetitions is currently too low for a statistically significant evaluation using rumen methanogens other than *M. ruminantium* M1. Further research is recommended to obtain sufficient statistical power to evaluate methane inhibition by PhaC-PeiR nanobeads on phylogenetically diverse rumen methanogens and validate the observed trends.

### Effect of nanobead purification on biological activity and methane inhibition

Based on existing protocols (described above), PhaC and PhaC-PeiR nanobeads were extracted from the respective *E. coli* production strains via sonication. Nanobeads obtained through this protocol were shown to be biological active and mediated methane inhibition against rumen methanogens. However, a tendency of PhaC-PeiR nanobeads was observed to form larger aggregates over time and during agitation which led to the hypothesis that PhaC-PeiR nanobeads may be more susceptible to mechanical stress. To test this hypothesis, the nanobead isolation protocol as modified by replacing the mechanical ultrasonic cell disruption with an

enzymatic cell lysis using lysozyme. The remainder of the extraction and modification protocol remained unchanged.

Biological activity against *M. ruminantium* M1 was first tested in growth assays (Figure 14). As shown earlier, nanobeads obtained via mechanical cell disruption exhibited the expected response, inhibiting M1 cell growth for four days after which a rise in optical density occurred. In contrast, PhaC-PeiR nanobeads obtained via the enzymatic lysozyme treatment displayed a significantly longer period of *M. ruminantium* M1 inhibition. M1 cells were inhibited for up to six days post inoculation (end of assay).

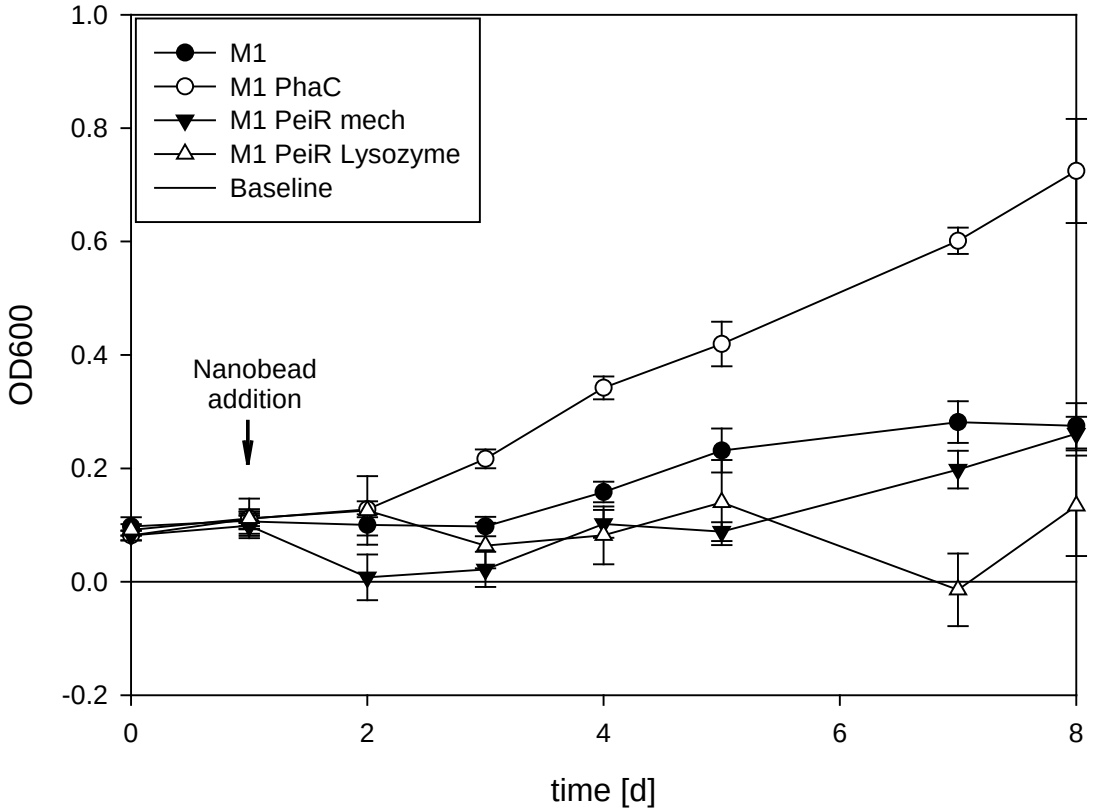


**Figure 14: Optical density assay testing the effect nanobead purification of PhaC-PeiR nanobeads on *M. ruminantium* M1.** M1: control (i), M1 cells only; M1 PhaC: control (ii), cells plus PhaC nanobeads; M1 PeiR mech: M1 cells with mechanically (*E. coli* production cells lysed via sonication) purified PhaC-PeiR nanobeads; M1 PeiR Lysozyme: M1 cells with enzymatically (*E. coli* production cells lysed via lysozyme treatment) purified PhaC-PeiR nanobeads; baseline: visual reference line for $OD_{600}$ = 0; vertical arrow, time point of nanobead addition. The assays were carried out in triplicate. Optical densities were corrected as described. Error bars represent the standard error calculated from uncorrected measured optical density values.

This enhanced level of biological activity was then validated through methane inhibition assays as described above. Methane production was calculated for *M. ruminantium* M1 cultures exposed to respective tailored nanobeads variants (Figure 15). M1 cultures with and without PhaC nanobeads produce methane throughout the time course of the assay. In accordance to results presented in Figure 12 A, PhaC-PeiR nanobeads obtained through mechanical disruption (PhaC-PeiR mech) mediated a complete methane inhibition for a short period of time, after which methane levels slowly recovered to control levels over the course of three days. In contrast, enzymatically purified PhaC-PeiR nanobeads (PhaC-PeiR Lysozyme) were able to completely inhibit methane production on day 4 and 5, while on days 7 and 8 methane was still reduced by 95 %.

The apparent tendency of PhaC-PeiR nanobeads to aggregate (whereas PhaC nanobeads retain their original state) may be due to a greater sensitivity to mechanical forces. However, an *in silico* analysis of the lytic enzyme PeiR (data not shown) revealed the presence of an N-terminal pseudo-murein binding repeat domain and a C-terminal peptidase domain. It is tempting to speculate that either domain may contribute to the observed aggregation. Mechanical forces (sonication or continued agitation) would then bring PeiR enzymes from different nanobeads in close proximity to each other for their respective domains to interact with each other.

These results demonstrated the potency of anti-methanogen nanobeads and the importance of optimising production procedures after the initial biological activities have been validated for a given tailored nanobead variety.

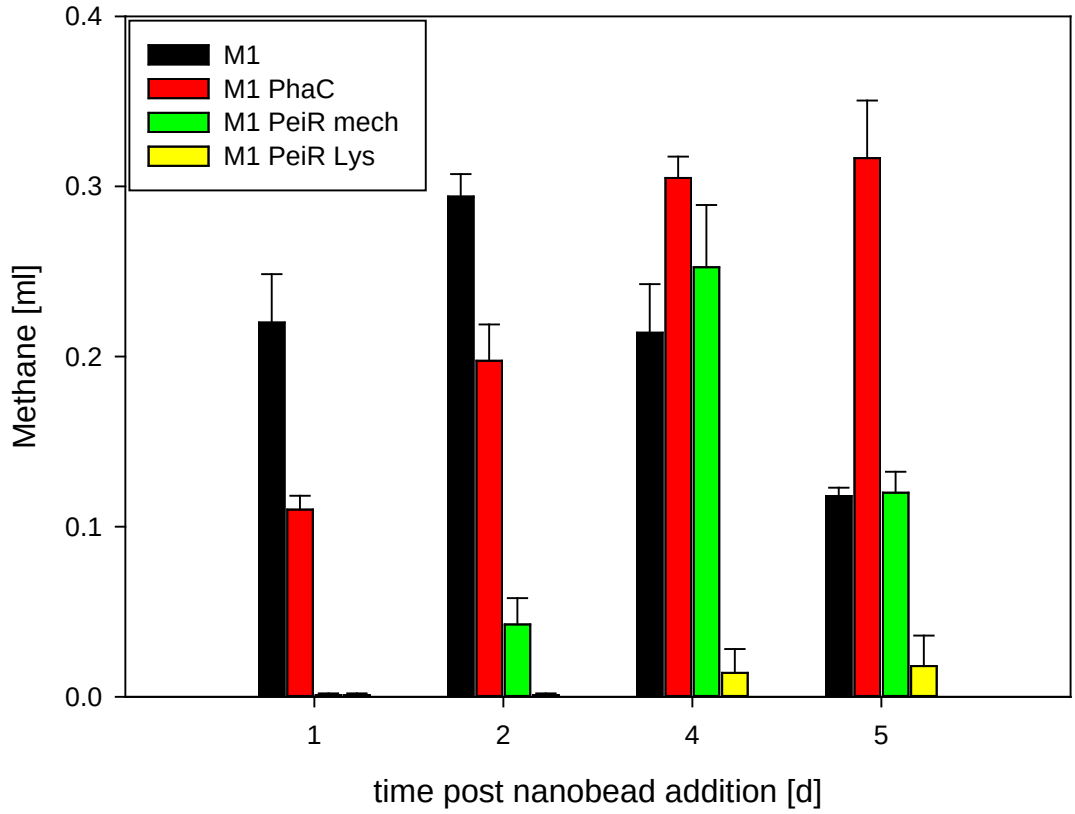


**Figure 15: Methane production in pure cultures in the presence of PhaC and PhaC-PeiR nanobeads.** PeiR mech: mechanically (*E. coli* production cells lysed via sonication) purified PhaC-PeiR nanobeads, PeiR Lysozyme: enzymatically (*E. coli* production cells lysed via lysozyme treatment) purified PhaC-PeiR nanobeads. Assays were carried out in triplicate. Error bars represent the standard error.

In summary, the enzymatic activity of PhaC-PeiR nanobeads and subsequent methane reduction was demonstrated not only against the original host strain *M. ruminantium* M1 but also against a number of other rumen methanogen strains. It was shown that by optimising the purification process, gains in biological activity can be achieved which may translate in production cost-savings of a commercial nanobeads based product. Additional independent experimental repetitions are required for some assays to increase the statistical power.

## MILESTONE 3: THE HALF-LIFE OF PHA NANOBEADS

### The half-life of PeiR-displaying nanobeads will be determined in pure methanogen cultures using direct fluorescence light microscopy assays

The rumen is a complex and highly active environment. It is feasible to hypothesise that bioplastics such as polyhydroxyalkanoates, the building blocks of PHA nanobeads, may be degraded rapidly in the presence of methanogens, rumen microbes, rumen growth media or rumen content/fluid. Therefore, the stability of PHA nanobeads was assessed using fluorescent microscopy assays, visually investigating the presence and structure of PHA nanobeads and quantifying nanobeads by integrating the measured fluorescence.

First, the presence and structure of PhaC and PhaC-PeiR nanobeads was investigated over four days in RM02 culture medium in the presence of growing *Methanobrevibacter ruminantium* M1 cells.

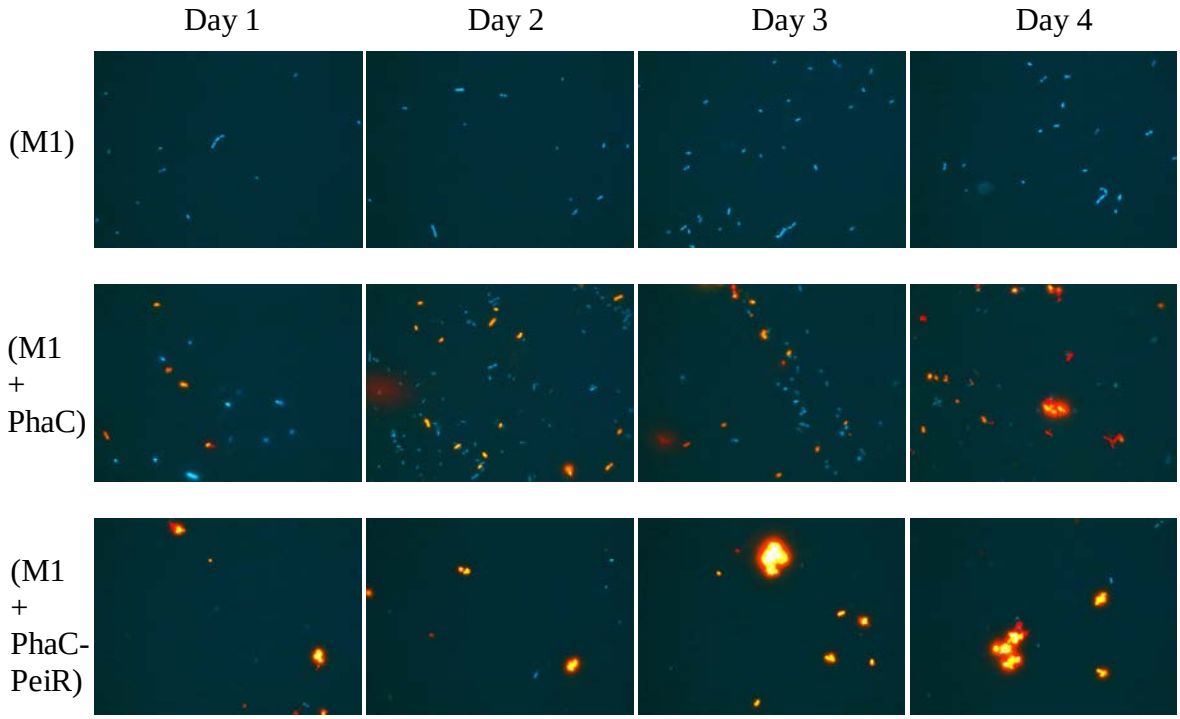


**Figure 16: Fluorescence microscopy of *M. ruminantium* M1 cells (M1), and M1 cells with added PhaC nanobeads (M1+PhaC) and with added PhaC-PeiR nanobeads (M1+PhaC-PeiR).** Samples were taken over four days post nanobead addition and representative slides selected. *M. ruminantium* M1 cells are shown in blue and Nile Red-loaded PhaC and PhaC-PeiR nanobeads appear in orange.

*M. ruminantium* M1 cultures were actively growing during the course of the assays and cell numbers increased accordingly (Figure 16, upper panel). The addition of PhaC nanobeads did not impact on cell growth and cell numbers increased in a similar manner to M1 without the addition of PhaC nanobeads. PhaC nanobeads appear to be structurally stable over four days in RM02 medium and in the presence of growing *M. ruminantium* M1 cells. No reduction in PhaC bead number was encountered and individual bead (clusters) did not show any signs of reduced fluorescence (Figure 16, middle panel). In contrast, PhaC-PeiR nanobeads revealed a tendency to form larger clusters over time (Figure 16, lower panel), albeit without a loss in fluorescence. Anti-methanogen activity was retained as evidenced by the reduction of *M. ruminantium* cell numbers visible in each field-of-view. This aggregation of PhaC-PeiR nanobeads was discussed earlier in Milestone 2.

### The half-life of PeiR-displaying nanobeads will be determined in mixed methanogen cultures using direct fluorescent light microscopy assays

The effect of PhaC-PeiR nanobeads on a co-culture between a methanogen and a rumen bacterium (and vice versa) was tested to investigate whether the presence of a rumen bacterial cells may impact on nanobead stability and activity. Similarly, PhaC-PeiR nanobeads may mediate a negative effect on rumen bacteria. Here, *Ruminococcus flavefaciens* FD1 was chosen as a co-culture partner to *M. ruminantium* M1. *Ruminococcus flavefaciens* FD1 is a cellulolytic rumen bacterium that takes part in ruminal plant fibre degradation. Growing cultures of *M. ruminantium* M1 and *Ruminococcus flavefaciens* FD1 were combined anaerobically and PhaC-PeiR nanobeads were added to the co-culture. After a 24 hour incubation period, the presence and absence of *M. ruminantium* M1 and *Ruminococcus flavefaciens* FD1 cells and the structural stability and fluorescence of PhaC-PeiR nanobeads were assessed via light-field and fluorescence microscopy (Figure 17).

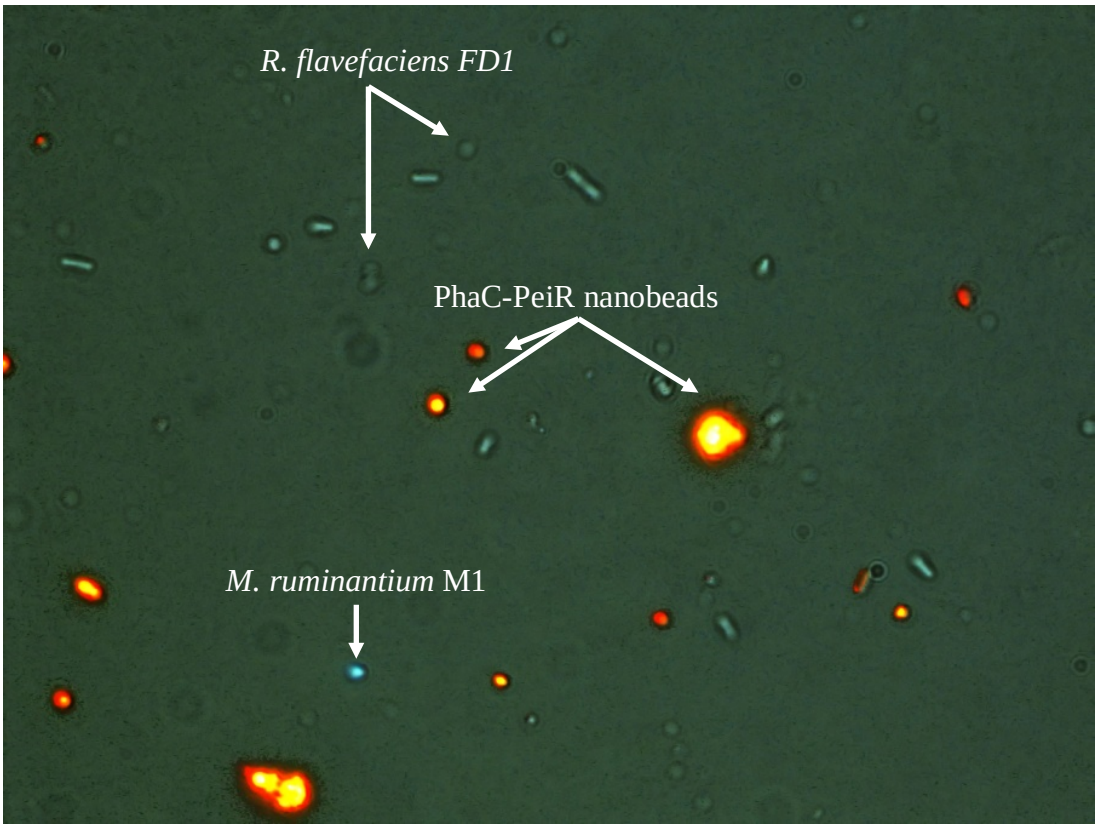


**Figure 17: Co-culture of *M. ruminantium* M1 and *Ruminococcus flavefaciens* FD1 in the presence of PhaC-PeiR nanobeads after 24 hours.** The picture is a composite image of light-field and fluorescent micrographs of the same field-of-view. Orange clusters indicate PhaC-PeiR nanobeads, blue fluorescing cocci represent *M. ruminantium* M1 cells and non-fluorescent cocci indicate the presence of *R. flavefaciens* FD1.

Almost no *M. ruminantium* M1 cells were found in the nanobead enriched co-culture, confirming the enzymatic anti-methanogen activity of PhaC-PeiR nanobeads. In contrast, no detrimental effects to cell numbers or cell morphology were observed for *R. flavefaciens* FD1, indicating that PhaC-PeiR beads are specific in their biological activity. Similarly, no structural degradation or a reduction in fluorescence of PhaC-PeiR nanobeads was detected. While other rumen microbes may exist that are able to readily degrade PHA nanobeads, these results indicate that PhaC nanobeads retain their structure and biological activity over at least 24 hr when exposed to cellulolytic microbes.

### The long-term stability of PhaC nanobeads will be determined in RM02 medium and clarified rumen fluid

To investigate the long term stability of PHA nanobeads, fluorescence of Nile Red-loaded PhaC nanobeads was measured over 49 days in RM02 medium and clarified rumen fluid. PhaC and PhaC-PeiR nanobeads are both made up of polyhydroxyalkanoate and are likely to degrade in similar ways. Because of the observed form-stability, PhaC nanobeads were chosen for this assay over PhaC-PeiR nanobeads.

Clarified rumen fluid was obtained as follows. Briefly, ~100 ml of fresh rumen contents were collected from cows with a fistulated rumen. The strained contents were centrifuged for 20 minutes at 10000 x *g*. While the procedure removed most microbes, the clarified rumen fluid was not filter sterilised and still contained viable microbes that may metabolise and grow during the duration of the assay.

50 mg of PhaC nanobeads was added to 50 ml of clarified rumen fluid or RM02 growth medium. The suspension was then incubated at room temperature over a course of 49 days. Over this time period, 1ml samples of bead suspension were taken at predefined intervals, spun down (16000 x *g* for 2 minutes) and stained with Nile Red as described above. Representative fluorescence micrographs of clarified rumen fluid and RM02 medium (control) and clarified rumen fluid/RM02 PhaC nanobead suspensions were taken. The overall fluorescence of Nile Red stained nanobeads was measured by integrating the measured fluorescence of individual nanobead (clusters) using the ImageJ software package.

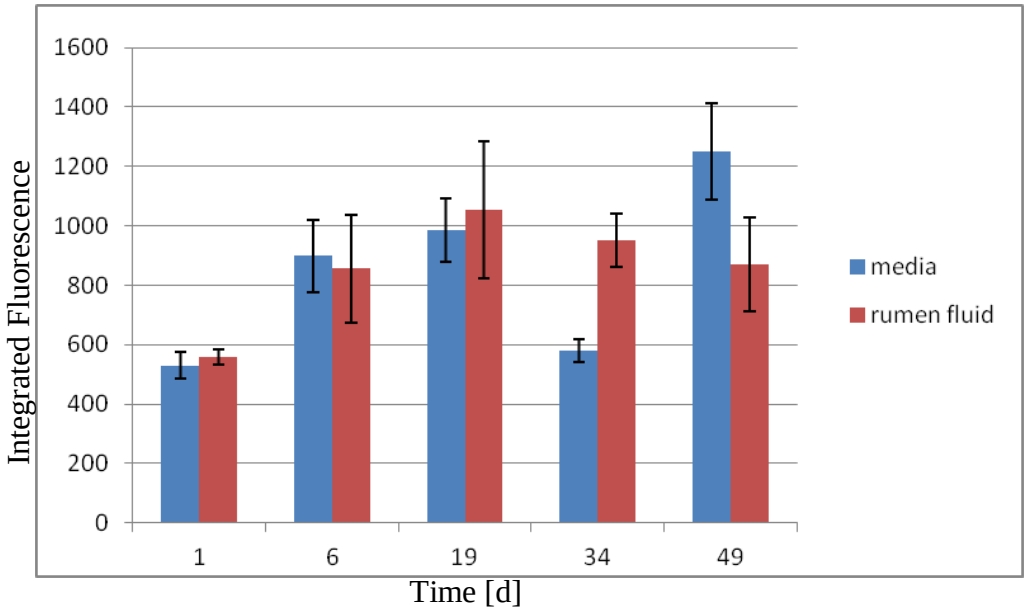


**Figure 18: Long term stability assay for PhaC nanobeads in RM02 medium (blue) and clarified rumen fluid (red).** Samples were taken at 1, 6, 19, 34 and 49 days post inoculation and fluorescence was integrated for a minimum of six replicates.

The long term stability assay revealed that PhaC nanobeads were stable over the entire period after an initial increase in fluorescence between day 1 and day 6 in both RM02 and in clarified rumen fluid (Figure 18)**.** While clarified rumen fluid represents only a proxy for active rumen content, it nevertheless contains solubilised enzymes and viable microbes that may be able to degrade PhaC nanobeads over time.

The results of the short term and long term stability assays provide evidence of the overall integrity and suitability of PHA nanobeads in the rumen environment. Subsequent experiments will investigate the stability and effect of PhaC and PhaC-PeiR nanobeads in rumen fermenters and in animal models.

## MILESTONE 4: EVALUATION OF SMALL MOLECULE INHIBITOR (SMI) UPTAKE

Small molecule inhibitors emerging from the chemogenomics programmes or already-published inhibitors will be evaluated *in silico* for nanobead uptake. Degrees of uptake will be correlated to known physicochemical SMI properties.

Polyhydroxyalkanoic nanobeads possess an amorphous hydrophobic core, contain either short-chain-length (3-5 carbons) or medium-chain length (six or greater carbons) monomers and can vary in their levels of crystallinity (between 30-70%) and size (50,000 to 1,000,000 Daltons) (3, 19, 24, 46, 47). Although nanobeads can be produced by a wide range of organisms and can incorporate a wide range of polymers (>150), production in *E. coli* is expected to be almost entirely of linear short-chain-length polyhydroxybutyrate (13, 26, 46, 47, 56). The overall size distribution and physical properties of the nanobeads can also be affected by the growth conditions during production (30, 41), the amount of expressed PhaC synthase (48) the surface proteins and cell division machinery (42, 44, 47). The industrial processing of nanobeads (e.g. cell harvesting, polymer purification) can also affect the final properties of the nanobeads (19, 41).

The predominant factor in controlling the ability to use nanobeads for targeted delivery of inhibitory compounds, however, will be the overall hydrophobicity of the compound. The presence of polar functional groups has the potential to cause compounds to become amphiphilic, and these would then be expected to be confined to the surface of the nanobeads (vastly reducing the storage capacity of the nanobeads). All of the above properties and factors can be expected to affect the rate and total uptake of the compound(s) that can be stored and rate of release of potential inhibitory compounds. If they are displayed on the surface, then the stability of the compounds may also be affected as they could become accessible to hydrolytic enzymes in the rumen. The pH in the rumen is fairly constant and will control the ionisation state of any ionisable functional groups of compounds and the 'equilibrium' concentrations in the bead and the rumen (21).

Another important factor in the use of nanobeads as a delivery mechanism is the concentration of the inhibitor itself, and the concentration required for significant methane reductions. Partner programs are currently aiming for an inhibitor that will reduce methane emissions by 20% using inhibitor concentrations that are effective at approximately 5-30 µM. This is based on cost constraints (the lower the effective concentration required likely means less overall cost), toxicology concerns (lowest possible concentrations are better) and delivery methods (bolus delivery over several months and these have a maximum size).

For the application as a rumen-based mitigation tool, the rate of release of inhibitors from nanobeads will be crucial for their effectiveness. Total turnover in the rumen varies but is generally between approximately 8-24 hours and this consists of two components, liquid and solid fractions, with liquid turnover occurring more quickly (17). Thus, the optimum release rate should be such that most of the compound is released from nanobeads within about 12-24 hours after introduction into the rumen when targeting free living methanogens. The rate of release of the compounds in the rumen will be affected by a number of feed and animal-based factors including rate of saliva production, age of the animal, pregnancy status, lactation status, water intake, rumination rate, the extent to which the particles are bound to or trapped in the gross fibre within the rumen, and feed type particle size and digestibility (17). The rate of release, as discussed above, will also be determined by the properties of the nanobeads themselves as a result of their cell-based production and subsequent purification. Proteins on their surface that are designed to bind to methanogens will differentially bind to separate clades

of rumen methanogens, such as *Methanobrevibacter* and *Methanosphaera* potentially affecting the rumen ecology of compound release.

Predicting the hydrophobicity of compounds, usually defined as the partitioning of the compound between water and octanol (logP; log $P_{octanol/water}$), has been intensively investigated by the pharmaceutical industry for a several decades. For example, the ZINC database contains over 22,000,000 purchasable compounds and the entire database can be screened based on calculated logP values. Other parameters relevant to solubility prediction that can be searched include desolvation energies and molecular mass (11, 38). Despite the wide range of predictors and servers for predicting solubility and a large published data of the solubility of compounds, experimental data of solubilities is compound-dependent. Companies such as Sigma-Aldrich will often supply solubility data in water and organic solvents in many instances. In addition, there is plethora of readily-accessible solubility data in worldwide databases and publications.

However, there are likely to be instances in the future where the solubility of a compound and its derivatives will be unknown and have to be experimentally determined. There are relevant general indices for hydrophobicity in drug development that have been described. One is the number of aromatic rings (21, 49). Rules for this property include: more than three aromatic rings correlates with poorer drug development prospects (via poorer solubility); and the effect of increasing ring count effects varies dependent on the ring type >carboaromatics >>heteroaromatics >carboaliphatics >heteroaliphatics, with heteroaliphatics often producing a beneficial effect. The above 'rules' circumscribe to some extent the types of molecules that would have the highest potential for use in the rumen.

The pharmaceutical industry has in recent years being investigating the use of PHA nanobeads as drug delivery systems (19, 52, 58). This is an analogous approach to the use of nanobeads as a targeted inhibitor delivery system for the rumen, except that the rumen is virtually anaerobic. In one study, rhodamine B isothiocyanate was used as a dye (similar to using Nile Red) and high loadings (75%) were achieved in beads between 150-250 nm in diameter (58). The beads were taken up by macrophages and the dye released over a period of at least 20 days, and was independent of the properties of the type of bead (polyhydroxybutyrate, polyhydroxyhexanoate or polylactic acid) and their size. Rhodamine B isothiocyanate was also used in a similar study. In this example the beads were prepared by thorough mixing of the beads with the dye in a ratio of 1:50 (dye to bead on a w/w basis) in dichloromethane (59). In another study, PHB-polyhydroxyhexanoate beads were used to deliver the poorly water-soluble anti-cancer drug etoposide (31). Interestingly, the drug loading ratio of the beads was strongly affected by the drug/polymer ratio. Drug content is calculated based on weight ((mg of drug loaded divided by mg bead) ×100). The drug content increased from 2.92% to 8.77% when the drug loading increased from 1/0.125 to 1/0.5. An additional finding of significance was that release was two-stage with an initial burst of as much as 25% of the compound (8) followed by a longer slow release. It has been hypothesised that the initial burst was due to release of the drug that was close to the surface of the beads, and the slower released drug was from the interior of the beads (8, 31). Budhian (7) has suggested that increasing hydrophobicity of the polymer will reduce the initial release rate and extend the total period of release. In an earlier study the antibiotic rifampicin (slightly soluble in water at 25°C: 2.5 mg/ml, pH 7.3) was used to load larger PHB nanobeads (5-100 microns). High drug loadings were achieved (407 mg drug/g of bead) (28). The large majority of the rifampicin (90%) was released within 24 hours. The release rate and loading rate for rifampicin is about what is needed for application of nanobeads in the rumen. In yet another study by Lu et al. 2011 (35) with PHB nanobeads loaded with the Pi3K inhibitor TGX221 (solubility <1 mg per ml in water; 12 mg per ml in DMSO; <1 mg per ml ethanol) 30%, 50% and 60% release was achieved after 30, 50 and 140 hours, respectively using ~200

nm nanobeads. Based on these few studies it would seem that a compound that is soluble at about 1-2 mg/ml in water is about the right solubility for delivery into the rumen.

Mathematical models of drug delivery using nano-technologies are predominantly based on diffusional mass transport. Basic factors in these models include the initial drug concentration:drug solubility ratio, and the geometry of the releasing particles (e.g. spherical, cylindrical) (54). Siepmann and Siepmann (53) listed 22 phenomena (most of these physicochemical effects) that could affect drug release from drug delivery systems, and of these the following are potentially relevant to nanobeads: penetration of acids, bases, salts and hydrophobic compounds into the beads (particularly the latter, possibly volatile fatty acids which are at high concentrations in the rumen), degradation or transformation of compounds at the surface by chemical reactions (e.g. by reduction or reaction with reactive molecules in the rumen) and/or hydrolytic enzymes, variations in expected release rates due to changes due to swelling of the beads and exceeding the solubility of the compound within the bead leading to altered release rate profiles.

Although PHA nanobeads are comprised of polar monomers (e.g. β-hydroxybutyrate), they are described as having an amorphous hydrophobic core, and can be solubilised in a variety of organic solvents (55). They are more soluble in chloroform than acetone (55). Nile red has been used as an effective tool for examining nanobeads in cells and during their processing using optical microscopes. Nile red is very insoluble in water (>1 μg $ml^{-1}$; (20, 27)).

Methanogens have been examined in numerous studies over three decades in a variety of study types including: phylogenetic, ecological, genetic, biochemical, biotechnological and agricultural. Most of these studies did not target rumen methanogens. However, as part of the PGgRc Meth0701 program, many of the available published inhibitors were tested against *Methanobrevibacter ruminantium* (50). However, most of these were not inhibitory to *M. ruminantium* at low enough concentrations to warrant further examination. The compounds that were sufficiently inhibitory were: gramicidin (an ionophore), pseudomonic acid (also called mupirocin targeting isoleucyl-tRNA synthetase), metronidazole (targeting pyruvate oxidoreductase), puromycin (peptidyl transfer in translation), and pravastatin (HMG CoA reductase in lipid synthesis). Due to the likely effects on fibre-degrading bacteria or toxicolgical effects on the host animal metronidazole, puromycin and pseudomonic acid are unlikely to be of use in the rumen. Gramicidin has been used before in rumen *in vitro* tests (80 mg/day) and in animal trials at low dose rates (22, 23). It is an ionophore similar to the widely used monensin as a growth promoter (51). Statins have previously been shown to inhibit rumen methanogens at low concentrations (37, 57). The ATPase of *M. ruminantium* has been examined and eight inhibitors were tested, most of which were active in the 1-100 μM range, however, none of these are specific for methanogens (36). The enzyme catalysing the first reaction in methanopterin synthesis (a methanogen cofactor), RFA-P synthase has been screened for inhibitors by (15) and three compounds inhibited growth of a methanogen at 100 μM, or below (one at 100 nM). When the 118 potentially inhibitory compounds were tested in rumen fluid based *in vitro* assays only two compounds showed partial activity (reduction in methane production) (4). Most of the compounds were sufficiently water soluble to not require nanobead delivery.

In addition, some plant extracts have been found to reduce methane emissions, however, few attempts have been made to identify which enzymes might have been the target of the active ingredient(s) (10). In particular, allicin, diallyl sulphide, diallyl disulfide and allyl mercaptan, active components of garlic, have raised interest in their use as mitigation agents (9, 10). Treatment with 300 mg/L using diallyl disulfide and allyl mercaptan caused reduction in methane of 68.5% and 19.5%, respectively. Diallyl disulfide and allyl mercaptan are both

insoluble in water and therefore would not be good candidates for use in nanobeads (release rate likely to be too slow), although derivatives could be investigated that might overcome these limitations. Anthraquinone has been patented for use as an anti-methanogen agent in the rumen and studied in 5 publications (16, 18, 32-34), and is poorly soluble in water (0.084 mg per litre at 20 °C). Anthraquinone represents a strong candidate for validation of the use of nanobeads, although its solubility might be such that release rates will be slower than optimal for use in the rumen (similar to Nile Red where 20 days were required for release). This could potentially be overcome by the use of derivatives that increase the solubility of anthraquinone without reducing its effectiveness.

Partner organisation programs (PGgRc Meth0701, NZAGRC Objective 1.4, GPLER 1 (96-well plate screening)) for the development of inhibitors for use in the rumen have identified numerous 'hit' compounds that inhibit either methanogen-specific enzymes or pure cultures of methanogens. Most of these are active at low enough concentrations against pure cultures of methanogens and will be tested in the coming months in rumen *in vitro* assays. Currently, three compounds have sufficient activity in rumen fluid-based assays to warrant further investigation (active against methanogens in pure culture in the 5-100 µM range), and one of these has been tested in an animal trial, but showed no effect (most likely due to low solubility of the compound). However, the latter compound requires concentrations too high to be used in nanobeads.

### Suitable candidates will be tested for incorporation into nanobeads *in vitro*

Based on the evaluation of existing suitable methanogen inhibitors, anthraquinone (AQ) was selected as the most suitable candidate. To measure the uptake of AQ into PHA nanobeads, 0.5 mg of granules were suspended in 50 mM phosphate buffer pH 7.35. Anthraquinone was dissolved in DMSO at increasing concentrations (0.1 mg/ml, 1 mg/ml, 10 mg/ml) and 100 µl of each solution added to the nanobead suspension. An aqueous phase was added by supplementing 990 µl of phosphate buffer. The aqueous phase facilitated the uptake of the hydrophobic AQ into the lipophilic nanobead interior. Loaded nanobeads were washed twice in phosphate buffer before being resuspended in 1 ml phosphate buffer.

Anthraquinone uptake was found to be dose dependent in a non-linear fashion (Figure 19). Optimal loading capacities were observed at an AQ concentration of 1 mg/ml. Greater concentrations did not result in significantly higher nanobead loading, whereas between 0.1 mg/ml and 1 mg/ml a proportional increase was observed.
As pointed out above, minimal inhibitory concentrations required for effective methanogen inhibition may be greatly influenced not only by the total amount of inhibitor present in PHA nanobeads, but also in their ability to deliver these compounds directly to methanogen cells. Such a close vicinity between inhibitor and target cells may greatly reduce the minimal dosage require and may be achieved by creating tailored nanobeads displaying cell-surface binding proteins that specifically target and bind to methanogen cells.

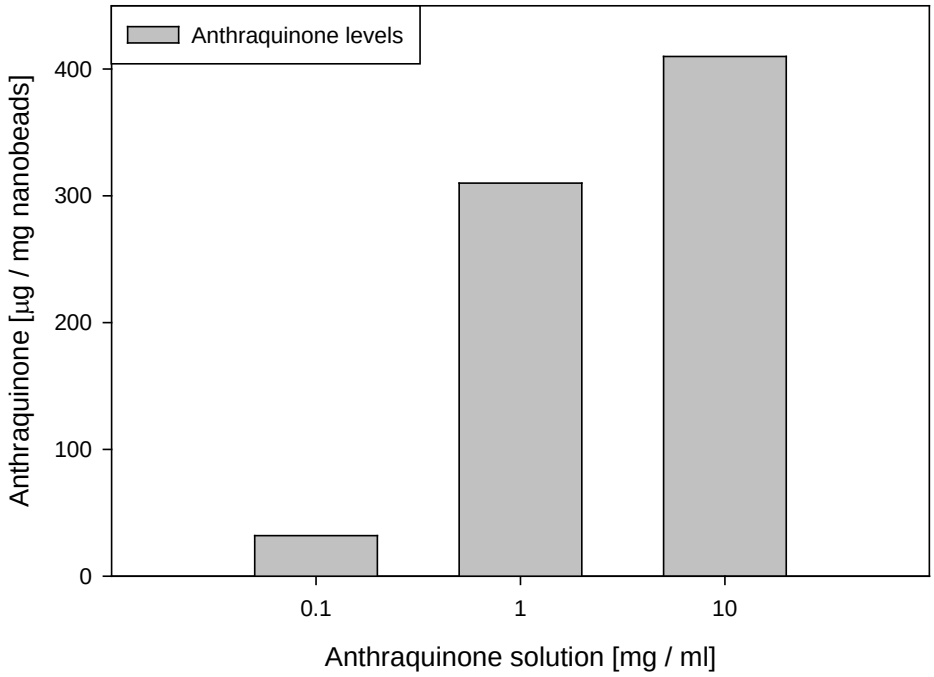


**Figure 19: Anthraqinone uptake of PHA nanobeads.** The amount of incorporated anthraqinone was measured by first solubilising loaded PHA nanobeads and then detecting levels of solubilised anthraquinone via HPLC.

# Summary and next steps

The two main aims of this SLMACC pilot programme were to test (a) whether archaeal proteins and enzymes can be displayed on the surface of PHA nanobeads produced in *E. coli* and (b) whether these tailored nanobeads display anti-methanogen activity.

A lytic enzyme (PeiR) that degrades cell walls of *M. ruminantium* M1 was successfully displayed on nanobeads as a PhaC-PeiR fusion protein. The enzyme was still active when displayed on the beads, as demonstrated by their anti-methanogen activity in growth assays and by reduced methane formation when they were added to pure methanogen cultures. The PhaC-PeiR nanobeads were active not only against the original host strain *M. ruminantium* M1, but also against two other rumen methanogens in pure cultures. This shows that active proteins can be displayed on the nanobeads and that these fusion proteins can act on methanogens.

PHA nanobeads displaying the PhaC-PeiR fusion protein were shown to be stable in the presence of methanogens and a methanogen-rumen bacterium co-culture in two short term experiments. A longer term assay then revealed no observable deterioration when PHA nanobeads were exposed to clarified (unsterile) rumen fluid over 49 days. This indicates that nanobeads may be structurally stable in the rumen environment. It remains to be shown how long the fused proteins/enzymes remain active *in vitro* / *in vivo* and that nanobeads can be retained in the rumen long enough to have an impact on methanogens.

To test whether PHA nanobeads could take up a known methanogen inhibitor, nanobeads were successfully loaded with up to 400 µg of anthraquinone per mg of PHA nanobeads. This demonstrates that nanobeads can be loaded with a lipophilic inhibitor. The next step is to show that the inhibitors can be released at sufficient rates to inhibit methanogens. The intention is that by displaying proteins or enzymes that bind to methanogens, nanobeads can deliver inhibitors directly to methanogen cells.

Based on the outcomes of the SLMACC pilot programme, the research priorities are to evaluate the PhaC-PeiR nanobeads and other anti-methanogen nanobeads variants *in vitro* and *in vivo*. The aim will be to create a range of tailored anti-methanogen nanobeads active against the major rumen methanogen groups found in New Zealand ruminants and to test those individually and in combination in more complex rumen fermenters and in animal models.

High level objectives of this prioritised research include:

- Determine the minimal inhibitory concentration (MIC) and the inhibition kinetics of PhaC-PeiR nanobeads against *M. ruminantium* M1 in pure culture. Knowledge of the minimal amount of active nanobeads required to inhibit methanogens is needed to predict more accurately the optimal bead load *in vitro* and *in vivo*. The retention time of an individual nanobead in the rumen may be less than 24 hrs. Anti-methanogen activity must take place during this time period and the kinetic assays will determine the speed at which methanogens are inhibited.
- Scale up production of the proven anti-methanogen PhaC-PeiR nanobead variant and measure the degree and duration of changes in the methanogen population in rumen fermenters (Dr. Stefan Muetzel, Mitigas). Rumen fermenters are recognised and amenable proxy systems. PhaC-PeiR nanobeads can therefore be tested for structural integrity and anti-methanogen activity in a complex environment.
- Measure the retention time of tailored nanobeads in the rumen by developing an easily traceable reporter-nanobead variant. Amounts of nanobeads present in the rumen and in faeces will be evaluated. To impact on the level of rumen methanogens, PHA nanobeads

must retain their physical integrity and biological activity in the rumen environment over time.

- Expand the range of tailored anti-methanogen nanobeads by employing lytic enzymes that target a wider range of methanogens, cell wall binding proteins that will bind to different methanogens, and antibody binding proteins (link to vaccine programme, Dr. Neil Wedlock). Tailored nanobeads effective against different methanogen groups will maximise the targeted inhibitory effect in the rumen.
- Load nanobeads with further anti-methanogen small molecule inhibitors (link to chemogenomics programme, Dr. Ron Ronimus) and determine uptake and release kinetics. The amount of incorporated inhibitor and its subsequent release in the rumen are important factors for efficient methanogen inhibition.
- Validate new nanobead variants *in vitro* by using assays established in the SLMACC pilot programme and in rumen fermenters. Identify their respective level of anti-methanogen activity and range in pure cultures and complex systems. Each new tailored nanobead variant is likely to have a different optimal anti-methanogen spectrum. Knowledge of this spectrum will enable the composition of the most effective cocktail of tailored nanobeads to act in the more complex rumen simulations and in animal trials.
- Scale up production of the most active and effective anti-methanogen nanobead variants to volumes suitable for animal trials.
- Test the most promising nanobead combinations in animals for efficacy. PGgRc have already indicated direct support of animal testing in parallel to the proposed GPLER research programme.

Funding of NZD $750,000 was indicated through the GPLER Round 2. Based on this funding, a focused two year research programme (NZD $375k /pa) is proposed, prioritising to test PhaC-PeiR nanobeads up to a small scale animal trial investigating changes in the rumen methanogen community *in vivo*:

**Step 1**: Determine the minimal inhibitory concentration (MIC) and the inhibition kinetics of PhaC-PeiR nanobeads against a rumen methanogen in pure culture.

**Step 2**: Measure the degree and duration of changes in the methanogen population in rumen fermenters in a dose-dependent manner. Production of the proven anti-methanogen PhaC-PeiR nanobeads will be increased accordingly.

**Step 3**: Monitor the effect on PhaC-PeiR nanobeads on the rumen methanogen population *in vivo* during a small scale animal trial.

At the end of the two year research programme the effect of PhaC-PeiR nanobeads in the rumen on methanobrevibacteria (and possibly other rumen methanogens) will have been demonstrated. Future steps will then comprise the use of new tailored anti-methanogen nanobeads, small molecule inhibitors and anti-methanogen antibodies to develop an effective mixture of tailored nanobeads active against all dominant rumen methanogen groups. Knowledge of minimal inhibitory concentrations and respective nanobead kinetics in the rumen will facilitate financial feasibility models for subsequent commercialisation.

Reference list


1. **Amara, A. A., and B. H. Rehm.** 2003. Replacement of the catalytic nucleophile cysteine-296 by serine in class II polyhydroxyalkanoate synthase from Pseudomonas aeruginosa-mediated synthesis of a new polyester: identification of catalytic residues. The Biochemical journal **374:**413-421. doi: 10.1042/BJ20030431 BJ20030431 [pii].
2. **Amara, A. A., A. Steinbuchel, and B. H. Rehm.** 2002. In vivo evolution of the Aeromonas punctata polyhydroxyalkanoate (PHA) synthase: isolation and characterization of modified PHA synthases with enhanced activity. Appl Microbiol Biotechnol **59:**477-482. doi: 10.1007/s00253-002-1035-3.
3. **Barham, P. J.** 1992. Physical properties of poly(hydroxybutyrate) and copolymers of hydroxybutyrate and hydroxyvalerate. FEMS Microbiology Reviews **103:**289-298.
4. **Behlke, E., R. Dumitru, S. W. Ragsdale, J. M. Takacs, and J. L. Miner.** 2006. Inhbition of methanogenesis in rumen fluid cultures. Nebraska Beef Cattle Report, University of Nebraska **83**.
5. **Blatchford, P. A., C. Scott, N. French, and B. H. Rehm.** 2012. Immobilization of organophosphohydrolase OpdA from Agrobacterium radiobacter by overproduction at the surface of polyester inclusions inside engineered Escherichia coli. Biotechnol Bioeng **109:**1101-1108. doi: 10.1002/bit.24402.
6. **Brandl, H., R. A. Gross, R. W. Lenz, and R. C. Fuller.** 1988. Pseudomonas oleovorans as a Source of Poly(beta-Hydroxyalkanoates) for Potential Applications as Biodegradable Polyesters. Appl Environ Microbiol **54:**1977-1982.
7. **Budhian, A., S. J. Siegel, and K. I. Winey.** 2008. Controlling the in vitro release profiles for a system of haloperidol-loaded PLGA nanoparticles. Int J Pharm. **346:**151-159.
8. **Budhian A, S. S., Winey KI.** 2008. Controlling the in vitro release profiles for a system of haloperidol-loaded PLGA nanoparticles. Int J Pharm. **346:**151-159.
9. **Busquet M, C. S., Ferret A, Carro MD, Kamel C.** 2005. Effect of garlic oil and four of its compounds on rumen microbial fermentation. J Dairy Sci. **88:**4393-4404.
10. **Busquet M, C. S., Ferret A, Kamel C.** 2006. Plant extracts affect in vitro rumen microbial fermentation. J Dairy Sci. **89:**761-771.
11. **Castellano, B. M., and D. K. Eggers.** 2013. Experimental support for a desolvation energy term in governing equations for binding equilibria. J Phys Chem B. **117:**8180-8188.
12. **Choi, J.-i., and S. Y. Lee.** 1997. Process analysis and economic evaluation for Poly(3-hydroxybutyrate) production by fermentation. Bioprocess and Biosystems Engineering **17:**335-342. doi: 10.1007/s004490050394.
13. **Dawes, E. A.** 1988. Polyhydroxybutyrate: an intriguing biopolymer. Biosci Rep. **8:**537-547.
14. **Dijkstra, J., J. M. Forbes, and J. France.** 2005. Quantitative Aspects of Ruminant Digestion and Metabolism Second edition ed. CABI.
15. **Dumitru, R., et al.** 2003. Targeting methanopterin biosynthesis to inhibit methanogenesis. Appl Environ Microbiol **69:**7236-7241.
16. **Ebrahimia SH, M. M., Singhal KK, Miri VH, Tyagi AK.** 2011. Evaluation of complementary effects of 9,10-anthraquinone and fumaric acid on methanogenesis and ruminal fermentation in vitro. Arch Anim Nutr. **65:**267-277.
17. **Firkins, J. L., M. S. Allen, B. S. Oldick, and N. R. St-Pierre.** 1998. Modeling ruminal digestibility of carbohydrates and microbial protein flow to the duodenum. J Dairy Sci. **81:**3350-3369.

18. **Garcia-Lopez, P. M., L. J. Kung, and J. M. Odom.** 1996. In vitro inhibition of microbial methane production by 9,10-anthraquinone. J Anim Sci. **74:**2276-2284.
19. **Grage, K., et al.** 2009. Bacterial polyhydroxyalkanoate granules: biogenesis, structure, and potential use as nano-/micro-beads in biotechnological and biomedical applications. Biomacromolecules **10:**660-669. doi: 10.1021/bm801394s.
20. **Greenspan, P., and S. D. Fowler.** 1985. Spectrofluorometric studies of the lipid probe, nile red. J Lipid Res. **26:**781-789.
21. **Hill AP, Y. R.** 2010. Getting physical in drug discovery: a contemporary perspective on solubility and hydrophobicity. Drug Discov Today. **15:**648-655.
22. **Hino T, S. H., Miwa T, Kanda M, Kumazawa S.** 1994. Effect of aibellin, a peptide antibiotic, on propionate production in the rumen of goats. J Dairy Sci. **77:**3426-3431.
23. **Hino T, T. K., Kanda M, Kumazawa S.** 1993. Effects of aibellin, a novel peptide antibiotic, on rumen fermentation in vitro. J Dairy Sci. **76:**2213-2221.
24. **Jacquel, N., C.-W. Lo, H.-S. Wu, Y.-H. Wei, and S. S. Wang.** 2007. Solubility of polyhydroxyalkanoates by eperiment and thermodynmaic correlations. . Thermodynamics **53:**2704-2714.
25. **Jahns, A. C., and B. H. A. Rehm.** 2009. Tolerance of the Ralstonia eutropha Class I Polyhydroxyalkanoate Synthase for Translational Fusions to Its C Terminus Reveals a New Mode of Functional Display. Applied and Environmental Microbiology **75:**5461-5466. doi: 10.1128/aem.01072-09.
26. **Jendrossek, D.** 2009. Polyhydroxyalkanoate granules are complex subcellular organelles (carbonosomes). . J Bacteriol. **191:**3195-3202.
27. **Jose, J., and K. Burgess.** 2006. Syntheses and properties of water-soluble Nile Red derivatives. J Org Chem. **71:**7835-7839.
28. **Kassab AC, X. K., Denkbaş EB, Dou Y, Zhao S, Pişkin E.** 1997. Rifampicin carrying polyhydroxybutyrate microspheres as a potential chemoembolization agent. J Biomater Sci Polym Ed. **8:**947-961.
29. **Keshavarz, T., and I. Roy.** 2010. Polyhydroxyalkanoates: bioplastics with a green agenda. Current Opinion in Microbiology **13:**321-326. doi: 10.1016/j.mib.2010.02.006.
30. **Khanna, S., and A. K. Srivastava.** 2006. optimization of nutrient feed concnetration and addition time for production of poly (B-hydroxybutyrate). Enzyme and Microbial Biotechnology **39:**1145-1151.
31. **Kılıçay E, D. M., Türk M, Güven E, Hazer B, Denkbas EB.** 2011. Preparation and characterization of poly(3-hydroxybutyrate-co-3-hydroxyhexanoate) (PHBHHX) based nanoparticles for targeted cancer therapy. Eur J Pharm Sci. **44:**310-320.
32. **Kung L, B. J., Tavares JY.** 2000. Effect of various compounds on in vitro ruminal fermentation and production of sulfide. Animal Feed Science and Technology **84:**69-81.
33. **Kung L Jr, H. A., Bracht JP.** 1998. Inhibition of sulfate reduction to sulfide by 9,10-anthraquinone in in vitro ruminal fermentations. J Dairy Sci. **81:**2251-2256.
34. **Kung L Jr, S. K., Smagala AM, Endres KM, Bessett CA, Ranjit NK, Yaissle J.** 2003. Effects of 9,10 anthraquinone on ruminal fermentation, total-tract digestion, and blood metabolite concentrations in sheep. J Anim Sci. **81:**323-328.
35. **Lu, X.-Y., et al.** 2011. Sustained release of PI3K inhibitor from PHA nanoparticles and in vitro growth inhibition of cancer cell lines. Applied Microbiology and Biotechnology **89:**1423-1433. doi: 10.1007/s00253-011-3101-1.
36. **McMillan DG, F. S., Dey D, Schröder K, Aung HL, Carbone V, Attwood GT, Ronimus RS, Meier T, Janssen PH, Cook GM.** 2011. A1Ao-ATP synthase of Methanobrevibacter ruminantium couples sodium ions for ATP synthesis under physiological conditions. J Biol Chem. **286:**39882-39892.

37. **Miller, T. L., and M. J. Wolin.** 2001. Inhibition of growth of methane-producing bacteria of the ruminant forestomach by hydroxymethylglutaryl-SCoA reductase inhibitors. J Dairy Sci **84:**1445-1448.
38. **Mishra, H., N. Singh, T. Lahiri, and K. Misra.** 2009. A comparative study on the molecular descriptors for predicting drug-likeness of small molecules. Bioinformation. **13:**384-388.
39. **Parlane, N. A., et al.** 2012. Vaccines displaying mycobacterial proteins on biopolyester beads stimulate cellular immunity and induce protection against tuberculosis. Clin Vaccine Immunol **19:**37-44. doi: CVI.05505-11 [pii] 10.1128/CVI.05505-11.
40. **Parlane, N. A., D. N. Wedlock, B. M. Buddle, and B. H. A. Rehm.** 2009. Bacterial Polyester Inclusions Engineered To Display Vaccine Candidate Antigens for Use as a Novel Class of Safe and Efficient Vaccine Delivery Agents. Applied and Environmental Microbiology **75:**7739-7744. doi: 10.1128/aem.01965-09.
41. **Penloglou, G., C. Chatzidoukas, and C. Kiparissides.** 2012. Microbial production of polyhydroxybutyrate with tailor-made properties: an integrated modelling approach and experimental validation. Biotechnol Adv. **30** 329-337.
42. **Peters, V., D. Becher, and B. H. Rehm.** 2007. The inherent property of polyhydroxyalkanoate synthase to form spherical PHA granules at the cell poles: the core region is required for polar localization. J Biotechnol **132:**238-245. doi: S0168-1656(07)00187-3 [pii] 10.1016/j.jbiotec.2007.03.001.
43. **Peters, V., and B. H. Rehm.** 2006. In vivo enzyme immobilization by use of engineered polyhydroxyalkanoate synthase. Appl Environ Microbiol **72:**1777-1783. doi: 72/3/1777 [pii] 10.1128/AEM.72.3.1777-1783.2006.
44. **Peters, V., and B. H. Rehm.** 2005. In vivo monitoring of PHA granule formation using GFP-labeled PHA synthases. FEMS Microbiol Lett **248:**93-100. doi: S0378-1097(05)00319-8 [pii] 10.1016/j.femsle.2005.05.027.
45. **Philip, S., T. Keshavarz, and I. Roy.** 2007. Polyhydroxyalkanoates: biodegradable polymers with a range of applications. Journal of Chemical Technology & Biotechnology **82:**233-247. doi: 10.1002/jctb.1667.
46. **Rehm, B. H.** 2010. Bacterial polymers: biosynthesis, modifications and applications. Nat Rev Microbiol **8:**578-592. doi: nrmicro2354 [pii] 10.1038/nrmicro2354.
47. **Rehm, B. H.** 2007. Biogenesis of microbial polyhydroxyalkanoate granules: a platform technology for the production of tailor-made bioparticles. Curr Issues Mol Biol. **9:**41-62.
48. **Rehm, B. H.** 2003. Polyester synthases: natural catalysts for plastics. Biochem J. **376:**15-33.
49. **Ritchie TJ, M. S.** 2009. The impact of aromatic ring count on compound developability--are too many aromatic rings a liability in drug design? Drug Discov Today. **14:**1011-1120.
50. **Ronimus, R. S., and D. Dey.** 2011. Effect on the growth of the rumen methanogen Methanobrevibacter ruminantium by antibiotics, mutagens and known antimicrobial compounds New Zealand Microbiological Society.
51. **Russell JB, S. H.** 1989. Effect of ionophores on ruminal fermentation. Appl Environ Microbiol. **55:**1-6.
52. **Shi J, V. A., Farokhzad OC, Langer R.** 2010. Nanotechnology in drug delivery and tissue engineering: from discovery to applications. Nano Lett. **10:**3223-3230.
53. **Siepmann J, S. F.** 2008. Mathematical modeling of drug delivery. Int J Pharm. **364:**328-343.
54. **Siepmann J, S. F.** 2012. Modeling of diffusion controlled drug delivery. J Control Release. **161:**351-362.

55. **Terada M, M. R.** 1999. Determination of solubility parameters for poly(3-hydroxyalkanoates). Int J Biol Macromol. **25:**207-215.
56. **Wang, Q., Q. Zhuang, Q. Liang, and Q. Qi.** 2013. Polyhydroxyalkanoatic acids from structurally-unrelated carbon sources in *Escherichia coli*. Enzyme and Microbial Biotechnology **97:**3301-3307.
57. **Wolin, M. J., and T. L. Miller.** 2006. Control of rumen methanogenesis by inhibiting the growth and activity of methanogens with hydroxymethylglutaryl-SCoA inhibitors. . International Congress Series **1293:**131-137.
58. **Xiong, Y.-C., Y.-C. Yao, X.-Y. Zhan, and G.-Q. Chen.** 2010. Application of Polyhydroxyalkanoates Nanoparticles as Intracellular Sustained Drug-Release Vectors. Journal of Biomaterials Science, Polymer Edition **21:**127-140. doi: 10.1163/156856209x410283.
59. **Yao YC, Z. X., Zhang J, Zou XH, Wang ZH, Xiong YC, Chen J, Chen GQ.** 2008. A specific drug targeting system based on polyhydroxyalkanoate granule binding protein PhaP fused with targeted cell ligands. Biomaterials. 2008 Dec;29(36):. doi: 10.1016/j.biomaterials.2008.09.008. **29:**4823-4830.
60. **Yuan, W., et al.** 2001. Class I and III Polyhydroxyalkanoate Synthases from Ralstonia eutropha and Allochromatium vinosum: Characterization and Substrate Specificity Studies. Archives of Biochemistry and Biophysics **394:**87-98. doi: 10.1006/abbi.2001.2522.